Uniform Solution for Uniform Polyhedra*

Zvi Har'El

Department of Mathematics
Technion − Israel Institute of Technology
Haifa 32000, Israel
E-Mail: rl@math.technion.ac.il

ABSTRACT

An arbitrary precision solution of uniform polyhedra and their duals is presented. The solution is uniform for all polyhedra given by their kaleidoscopic construction, with no need to 'examine' each polyhedron separately.

1. Introduction.

Uniform polyhedra, whose faces are regular and vertices equivalent, have been studied since antiquity. Best known are the five Platonic solids and the 13 Archimedean solids. We then have the two infinite families of uniform prisms and antiprisms. Allowing for star faces or vertices, we have the four Kepler-Poinsot regular star polyhedra and a row of 53 nonconvex uniform polyhedra discovered in the 1880s and the 1930s. The complete set appeared in print for the first time in 1953, in a paper by Coxeter, Longuet-Higgins and Miller ([CLM], see also [S]).

Magnus Wenninger's delightful book *Polyhedron Models* [W1], which appeared in 1971 but since has been reprinted many times, contains photos and building instructions for cardboard models of these 75 uniform polyhedra. Reading the book, makes the mathematically minded reader wonder: How are the data for the models obtained? For example, what makes 1. 1600030093 the proper circumradius for a *great retrosnub icosidodecahedron*[1] with edge length two?

It is easy to check, that these data originate in [CLM, Table 7]. Some of the circumradii are exact, as they are given in terms of integers and radicals only, but few, as the one mentioned above, are given approximately, to ten decimal digits. This may be considered perhaps accurate enough, but if one wants to incorporate polyhedra in a computer modeling software (cf. [Hy]), one would prefer to get the numbers in an arbitrary precision, or in the maximum precision the computer can handle. Furthermore, one is interested in exact, or maximum precision, values of other geometric data, such as the dihedral angles of the polyhedra, and for these the only available data are for the regular and the convex cases, and are accurate to 1″ (cf. [CR, Table II] and [J, Table II]).

This problem was treated by Andrew Hume. His method is best described by a short quotation from his report [Hm]:

> *In general, the data are solutions of equations found by examining the polyhedra (for example [L, pp. 174-176]). The equations were solved at least three times using symbolic algebra systems...*

Uniform polyhedra for which symbolic algebra systems are useful are the so-called snub polyhedra, and the computations involve solving cubic or quartic equations. Hume's solutions were used to create a database of polyhedra, which is publicly available at *netlib@research.att.com*.

---

* In memoriam of my father, Gershon Har'El, who introduced me to spatial structures.

Geometriae Dedicata **47:** 57-110, 1993.

[1] This is the [W2] version of the polyhedron name.

Our approach is quite different. Rather then separately examining individual polyhedra, we suggest a uniform approach, which is easy to understand and easy to use, even with a hand-held calculator, and it eliminates the need for a database for uniform polyhedra and their duals, since the fast iterative algorithm may yield arbitrary precision data. Furthermore, it may be used in the same ease for convex as well as for nonconvex polyhedra (which are not treated by [Hm]). A computer program, called *kaleido* (cf. [Ha]) and publicly available at *ftp@ftp.math.technion.ac.il*, has been developed to compute the data of a uniform polyhedron (and its dual), given either the vertex configuration, i.e, the enumeration of the polygons appearing as faces incident at a vertex in the order in which they are found (cf. [CR, §2.9.2]), or the so-called *Wythoff symbol* which describes the kaleidoscopic construction of the polyhedron (cf. [CLM, §3]). *Kaleido* is also capable of computing the vertex and face coordinates and displaying a rotating wire-frame image of each polyhedron.

We would like to express our gratitude to H. S. M. Coxeter, Branko Grünbaum and Andrew Hume, for the very useful and enlightening comments.

2. The Fundamental System.

The *uniform solution* is based upon projecting the uniform polyhedron onto a concentric sphere, decomposing each n-sided tile in the spherical tiling into $2n$ congruent right-angled spherical triangles, setting the trigonometric equations and solving them iteratively. We shall explain the solution algorithm in the next section. Here, we discuss the procedure of identifying the fundamental triangles and setting the fundamental equations.

Let us assume, for the moment, that we are investigating a convex uniform polyhedron, such that each of its vertices is incident to m faces, with the ith face being a regular n_i-gon, customarily denoted by the *Schläfli symbol* $\{n_i\}$. The cyclic list $(n_1.\, n_2.\, \cdots .\, n_m)$ is the *vertex configuration*.

Projecting the polyhedron on a concentric sphere, we get a spherical tiling. Choose a vertex C, and let A_i, for $i = 1, \cdots, m$, be the incenter of the of the ith tile incident to C. Also, let B_i be the foot of the perpendicular from A_i to the arc separating the ith and $(i+1)$st tiles (the $(m+1)$st being identified as the first). In fact, the spherical polygon $A_1A_2\cdots A_m$ is the *prototile* of the *dual tiling* (cf. [GS, §1.2]). Also, the planar polygon $B_1B_2\cdots B_m$ is the so called *vertex figure* at C (cf. [C, §2.1]).

This way, we decompose the spherical tiling into right-angled spherical triangles, called the *fundamental triangles*: At each vertex C we get $2m$ fundamental triangles, arranged in congruent pairs $A_iB_{i-1}C$ and A_iB_iC, for $i = 1, \cdots, m$. The set of fundamental triangles will be called the *fundamental triangulation*. Note that the same triangulation also arise from a similar decomposition of the dual tiling (cf. [GS], section 2.7).

Denote the sides and the angles of A_iB_iC by a_i, b_i, c_i, α_i, $\frac{\pi}{2}$, γ_i, in the obvious manner (the right angle is at B_i). From the definition of A_i, and the regularity of the face, we easily see

$$n_i\alpha_i = \pi, \tag{1}$$

for $i = 1, \cdots, m$. Furthermore, if we consider the angles of the fundamental triangles meeting at C, we get

$$\sum \gamma_i = \pi. \tag{2}$$

Finally, we use the fact that the edge CB_i is shared by the two neighboring fundamental triangles A_iB_iC and $A_{i+1}B_iC$, and get $a_i = a_{i+1}$. Thus, all the a_i's are equal, and the common value, say a, satisfies

$$\cos a = \frac{\cos\alpha_i}{\sin\gamma_i} \tag{3}$$

for $i = 1, \cdots, m$, as may be easily deduced from the spherical law of cosines, or from Napier's second rule of circular parts (cf. [M]).

Thus, we get a system of $2m+1$ simultaneous equations (where $m+1$ are linear and m are trigonometric) in the $2m+1$ unknowns α_i, γ_i and $\cos a$. We name it the *fundamental system*, and we shall describe its solution in the next section.

Once the fundamental system has been solved, the rest of the sides of the fundamental triangles may be solved using similar formulas:

$$\cos c_i = \frac{\cos \gamma_i}{\sin \alpha_i}$$

$$\cos b_i = \frac{1}{\tan \alpha_i \tan \gamma_i}$$

The solution of the fundamental triangles reflects directly on the problem of finding all the metrical properties of the uniform polyhedron: Let $R, \rho, r_i, l, h_i, \theta_i, \phi_i$, be respectively the circumradius (the distance from the center to a vertex), the midradius (the distance from the center to an edge), the inradius (the distance from the center to the face), the semiedge, the facial inradius, the facial angle and the dihedral angle (the angle between the the i'th and the $i+1$'st faces). Then it is not hard to verify that $\frac{\rho}{R} = \cos a$, $\frac{r_i}{\rho} = \cos c_i$, $\frac{l}{\rho} = \tan a$, $\frac{h_i}{r_i} = \tan c_i$, $\theta_i = \pi - 2\alpha_i$, $\phi_i = \pi - c_i - c_{i+1}$.

The construction described above can be easily adjusted to accommodate nonconvex uniform polyhedra[2]. Such polyhedra may have star polygons as faces, or have the faces meeting at a vertex surround it more than once. In the former case n_i may be taken fractional (with the denominator being the *density* of the star face, cf. [C]), and in the latter case the right hand side of (2) is a multiple of π (with the multiplier being the density of the star vertex). Finally, nonconvex polyhedra may have *retrograde* faces, as follows: Choose an arbitrary orientation on the circumcircle of the vertex figure. The i'th face is said to be retrograde if the shorter of the the two arcs connecting B_{i-1} to B_i is oppositely oriented. (We assume that at least one face is not retrograde!) In this case we will represent a retrograde $\{n\}$ by an $\{n'\}$, with $n' < 2$ satisfying $\frac{1}{n} + \frac{1}{n'} = 1$. This will make $\alpha' = \pi - \alpha$ obtuse, and $\gamma' = -\gamma$ negative, as required. We will reiterate on these adjustments in the next section.

It is worthwhile to note that [CLM], p. 420, utilize the circumcircle of the vertex figure and elementary plane trigonometry to derive a set of equations which is essentially identical to our fundamental system. They are also able to obtain, by elimination, a single quartic equation, and use it to to prove that their list of snub polyhedra is complete (cf. [CLM], table 4). However, from our point of view, such derivation obscures the tight relationship between uniform polyhedra and their fundamental triangulations, a relationship which will be instrumental in section 4. Furthermore, the elimination method is not as uniform as the iterative solution to be presented in section 3, since it has to be carried out afresh for each polyhedron type and requires quite a few symbolic manipulations, algebraic and trigonometric.

3. The Iterative Solution.

We now describe the iterative solution of the fundamental system, based on well-known Newton's method for solving nonlinear equations. The general idea is to solve $2n$ of the unknown in terms of the $2n+1$'st, referred later as the *independent* unknown, and to compute the latter by iterative approximations. One of the problems in such an approach is the choice of the independent unknown, and we will attend to it shortly.

First, we notice that the α_i's are readily available from (1):

$$\alpha_i = \frac{\pi}{n_i} \tag{4}$$

for $i = 1, \cdots, m$.

Furthermore, once one of the γ_i's, say γ_1, is computed, all the rest are available from (3):

$$\cos a = \frac{\cos \alpha_1}{\sin \gamma_1} \tag{5}$$

$$\gamma_i = \arcsin\left(\frac{\cos \alpha_i}{\cos a}\right) \tag{6}$$

[2] The corresponding spherical tiling consists of *hollow tiles* in the sense of [GMS] (cf. [GS], section 12.3), and the fundamental triangulation be viewed as a multiple tiling of the sphere by triangles, or a triangulation of a Riemann surface (cf. [GS], section 12.4)).

for $i = 2, \cdots, m$.

Note that the inverse sine function in (6) has seemingly two values in the range $(0, \pi)$. However, it may be easily observed that at most one of the γ_i's may be obtuse, and we may assume, without any loss of generality, that γ_i, for $i = 2, \cdots, m$, are all acute.

Thus, (2) may be rewritten as

$$\delta = \pi - \sum \gamma_i = 0, \tag{7}$$

where δ is a well defined function of γ_1 only.

We recall Newton's method for solving the equation $f(x) = 0$: Choose an initial approximation to the root and then define a sequence of closer approximations using the recursion

$$\hat{x} = x - \frac{f(x)}{f'(x)} \tag{8}$$

Assume initially that the fundamental triangles are approximately planar. This motivates the initial approximation

$$\gamma_i = \frac{\pi}{2} - \alpha_{i.}$$

for $i = 1, \cdots, m$.

This certainly satisfies (5) and (6) (with $\cos a = 1$), but as these values for the γ_i's are smaller than in reality (as the sum of the angles in a spherical triangle exceeds π), δ in (7) will not vanish, but rather be a positive number, which motivates naming it the *excess function*. The iterative procedure will converge if we are able to make the excess arbitrarily small. It may be shown, at least empirically, that in order to guarantee convergence it is sometimes necessary to choose γ_1 as the biggest of the initial values, i.e., choose α_1 to be the smallest of the α_i's, or, in view of (4), choose n_1 to be the biggest of the n_i's.

This choice is the obvious the case for those polyhedra for which γ_1 turn to be obtuse, in view of our observation about the double-valuedness of the inverse sine function. Also, it may be shown that in the general case, this choice also guarantees a faster convergence than then any other choice. We'll see why it happens once we developed the recursion formula.

To use (8), we have to differentiate the excess function; we have from (7),

$$-\frac{d\delta}{d\gamma_1} = 1 + \sum{}' \frac{d\gamma_i}{d\gamma_1} \tag{9}$$

(with the prime denoting summation over the range $2, \cdots, m$). However, in view of (5) and (6),

$$\sin \gamma_i = \frac{\sin \gamma_1 \cos \alpha_i}{\cos \alpha_1}$$

which in turn implies, using logarithmic differentiation,

$$\frac{d\gamma_i}{d\gamma_1} = \frac{\tan \gamma_i}{\tan \gamma_1}. \tag{10}$$

Combining (7), (9) and (10) we get

$$-\frac{\delta}{\delta'} = \delta \frac{\tan \gamma_1}{\sum \tan \gamma_i}$$

(with summation again over the full range $1, \cdots, m$, and δ' is the derivative in (9)).

Finally, we arrive at the required recursion for γ_1:

$$\hat{\gamma}_1 = \gamma_1 + \delta \frac{\tan \gamma_1}{\sum \tan \gamma_i}$$

In practice, we notice that the faces meeting at a vertex are not necessarily different, thus we may group similar faces together, and adjust the above formulas to reflect the fact that at each vertex the polyhedron can have m_i faces each of which is a $\{n_i\}$, with $\sum m_i = m$. Furthermore, we handle retrograde faces

by orienting the vertex figure so that the the first, thus biggest, face is not retrograde. Thus, n_i is a positive rational, and m_i is a positive integer. d, the vertex density, is a non-negative integer.

To summarize, fundamental system

$$n_i\alpha_i = \pi$$

$$\sum m_i\gamma_i = \pi d$$

$$\frac{\cos\alpha_i}{\sin\gamma_i} = \cos a$$

where $n_1 = \max n_i$, has the following iterative solution algorithm:

Step 1.

Choose the initial approximation $\gamma_i = \frac{\pi}{2} - \alpha_i$, where $\alpha_i = \frac{\pi}{n_i}$.

Step 2.

Compute the excess $\delta = \pi d - \sum m_i\gamma_i$. If it is numerically small enough, finish. Otherwise, continue to step 3.

Step 3.

Compute the next approximation to the independent unknown γ_1 using the recursion

$$\hat{\gamma}_1 = \gamma_1 + \delta\,\frac{\tan\gamma_1}{\sum m_i\tan\gamma_i}$$

Step 4.

Compute $\cos a$ and γ_i, $i = 2, \cdots, m$, using

$$\cos a = \frac{\cos\alpha_1}{\sin\gamma_1}$$

$$\gamma_i = \arcsin\left(\frac{\cos\alpha_i}{\cos a}\right)$$

Step 5.

Return to step 2.

We want to make an observation about the convergence of this algorithm. The increment in γ_1 in step 3 may be very small even without the excess δ being small. This happens if the denominator $\sum m_i\tan\gamma_i$ is large, unless the numerator $\tan\gamma_1$ behaves similarly. In such cases the algorithm converges slowly or even diverges, and our choice for the independent unknown prevent them from occurring. By the way, choosing $\cos a$ as the independent unknown creates similar problems and although it looks plausible and perhaps more elegant (compare with the well known *Lagrange multipliers*), it should be avoided. A mathematically rigorous proof of convergence is out of the scope of this paper; We will have to be satisfied by empirical convergence for all the finitely many uniform polyhedra (cf. [CLM], [S]).

Note that in few exceptional cases, the direct approach fails. In these cases, it happens that the vertex density d is zero, and the faces incident at a vertex occur in several oppositely oriented pairs, and thus even the initial approximation satisfies the fundamental system, which is obviously impossible, since, as we already remarked, $\alpha_i + \gamma_i > \frac{\pi}{2}$ in a right-angled spherical triangle. It is interesting to note that these polyhedra are exactly those which cannot be constructed directly using the *Wythoff* construction, to be presented in the section 4. In section 5 we present an adjustment to the construction, which in turn leads to an adjustment to the fundamental system, which makes it possible to handle these exceptions.

4. The Kaleidoscope.

We start by discussing the *dihedral kaleidoscope*. It consists of two hinged planar mirrors. The reflections in these mirrors generate a group of isometries, which is finite if the dihedral angle of the kaleidoscope is a rational submultiple of π, i.e., of the form $\frac{\pi}{q}$, where q is a rational greater than one. We now

consider the meaning of these particular angles from additional points of view.

Intersect the kaleidoscope by a perpendicular plane, and choose a circle in this plane with center at the corner. The kaleidoscope encloses a circular arc, and we may ask for the cases in which repeated reflections of this arc in the mirrors produce a finite covering of the circle. It is easy to see that a d-fold covering obtained if $q = \frac{n}{d}$, where n and d are relatively prime positive integers, with $n > d$. In this case the the kaleidoscope generates D_n, the dihedral group of order $2n$, and the $\frac{\pi}{q} = \frac{\pi d}{n}$ arc consists of d copies of the fundamental domain of the group, a $\frac{\pi}{n}$ arc.

Now, put a point object in a general position on the enclosed arc. Then, repeated reflections in the mirrors will yield $2n$ points. which may naturally be viewed as the vertices of a $2n$-gon, where adjacent vertices belong to arcs which share an endpoint. Let the $2n$-gon be $C_1C_2\cdots C_{2n}$, where C_1 is the point object.

Note, that in two cases we get a smaller number of images: The first case is when $C_1 = C_2$ or $C_1 = C_{2n}$, which means that C_1 is a fixed point of one of the original reflections, or, geometrically, that the point object is located on one of the mirrors. Then, we get n pairs of coincident adjacent vertices, which means that n of the edges of the polygon are degenerate, and may be discarded. Thus, when the point object is located on one of the mirrors, we get regular n-gon, with density d, customarily denoted by $\{\frac{n}{d}\}$, i. e., $\{q\}$. Note, that if $\{q\}$ and $\{q'\}$ satisfy $\frac{1}{q} + \frac{1}{q'} = 1$, they are two oppositely oriented copies of the same polygon.

The other case is when $C_{n+1} = C_1$. This is only possible if the $n+1$st arc coincides with the first, but oppositely oriented. Thus, C_1 is located on the bisecting plane of the kaleidoscope, and the reflection in this plane belongs to to the dihedral group generated by the kaleidoscope. In this case we have no degenerate edges, but rather a regular n-gon which is transversed twice. As the density of the compound is d, d has to be even and each polygon has density $\frac{d}{2}$. Thus, when the point object is located on the bisector, we get a double $\{\frac{n}{(d/2)}\}$, i.e., a double $\{2q\}$. It is easy to check that if the point object is similarly located but the denominator d is odd, it traces a single regular $2n$-gon with density d, i.e., a single $\{2q\}$.

In all the other cases the polygon is an irregular $2n$-gon, however if we use only rotations (or any even number of reflections) then the polygon $C_1C_3\cdots C_{2n-1}$ is still regular, a $\{q\}$.

We now add a third mirror, and get the *trihedral kaleidoscope*, which consists of three concurrent planar mirrors. The problem of finding conditions on the dihedral angles for the kaleidoscope to generate a finite group of isometries was posed and solved by A. H. Schwarz in 1873. As we have already seen, it is necessary that these angles are rational submultiples of π, but however this is not sufficient. Intersecting the kaleidoscope by a sphere centered in its corner, Schwarz formulated the following problem: Enumerate all convex spherical triangles PQR, with angles $\frac{\pi}{p}$, $\frac{\pi}{q}$ and $\frac{\pi}{r}$ (p,q,r are all rational greater than one), with the property that when reflected in its sides any number of times, PQR produces a finite covering of the sphere. Such a triangle is called a *Schwarz triangle* and is denoted by the symbol (p q r). It may be shown that unless two of the angles are $\frac{\pi}{2}$ (in which case the kaleidoscope generates the dihedral symmetry group), p, q, and r may have as numerators the numbers 2, 3, 4 or 5, with the further stipulation that 4 and 5 cannot occur together. The denominator has to be smaller than the numerator, and this makes the number of nondihedral Schwarz triangles finite. A complete list of Schwarz triangles may be found in [C], table III, and in appendix I.

Putting a point object C in the Schwarz triangle PQR, it is now reflected repeatedly to produce a polyhedron, whose vertices are the images of the point object. As before, two vertices are considered adjacent if they belong to triangles which share an edge, and several vertices are incident to the same face if they belong to triangles which share a vertex. Note that as in the previous discussion, the polyhedron may be degenerate: Two images may coincide without a similar coincidence of the Schwarz triangles. This means that the polyhedron may be split into several, not necessarily distinct, polyhedra. This phenomenon is investigated in [CLM], and we will not discuss it here any detail (but see however section 5).

The kaleidoscopic construction of polyhedra is named after Wythoff (1918) who was the first to use it (in four dimensions, cf. [CLM], p. 406).

Assuming nondegeneracy, Wythoff construction is very useful in getting the topological invariants of the traced polyhedra, that is, the covering density D and the Euler characteristic χ. Both values can be easily computed for the for the multiple tiling of the sphere by Schwarz triangle: D may be found from the area of $(p\ q\ r)$ and the order g of the symmetry group generated by the reflection in its sides:

$$4\pi D = g(\frac{\pi}{p} + \frac{\pi}{q} + \frac{\pi}{r} - \pi),$$

or,

$$D = \frac{g}{4}(\frac{1}{p} + \frac{1}{q} + \frac{1}{r} - 1).$$

Note that the value of g is $4n$, 24, 48 or 120 if the group is n-fold dihedral, tetrahedral, octahedral or icosahedral, respectively. As pointed out in [CLM] (p. 412, 418, 425), this is also the correct value for the density of any polyhedron derivable from $(p\ q\ r)$, except for the cases where the spherical polyhedron possesses faces which are hemispherical or concave (i.e., bigger than a hemisphere). In the former case, the planar faces are incident at the center, and the density is not well-defined. In the latter case, the spherical and planar faces occur on two different sides of the center, and the density of the planar polyhedron may be computed by subtracting the density of the spherical polyhedron above from the number of concave faces (see the tables in appendix II; in our notation, a face is concave if γ is obtuse, see section 3).

The Euler characteristic relates V, the number of vertices, E, the number of edges, and F, the number of faces of any map drawn on a given closed surface by the famous Euler formula $V - E + F = \chi$. Here, we are considering a D-sheeted Riemann surface, which is triangulated by the Schwarz triangles, so that $F = g$, $E = \frac{3g}{2}$, and $V = V_p + V_q + V_r$, where V_q is the number of vertices with the angle $\frac{\pi}{q}$, i.e., $V_q = \frac{g}{2n_q}$, where n_q is the numerator of q. Thus, we get the formula

$$\chi = \frac{g}{2}(\frac{1}{n_p} + \frac{1}{n_q} + \frac{1}{n_r} - 1)$$

This value is also inherited by any non-degenerate polyhedron derivable from $(p\ q\ r)$ (see the tables in appendix II; see section 5 for the degenerate cases). It is very interesting to note that χ depends upon the numerators only. This means, for instance, that the convex Plato's icosahedron and the star-cornered Poinsot's great icosahedron, derivable from (2 3 5) and (2 3 $\frac{5}{2}$), have both Euler characteristic 2, and are thus homeomorphic as closed surfaces, although their densities are much different (1 for the former, 7 for the latter).

It is clear, that wherever we put a point C in the Schwarz triangle PQR, the traced polyhedron will be isogonal, i. e., all its vertices will be equivalent under the action of the isometry group generated by the three reflections. We will now discuss the positions of C which guarantee that the traced faces will be regular polygons, and study the corresponding spherical tiling and the fundamental triangulation and its triangular prototiles A_iB_iC. As before, $A_1A_2\cdots$ will be the prototile of the dual tiling, and $B_1B_2\cdots$ the vertex figure.

4.1. C **is at the vertex** P **of** PQR**.**

Let A_1 and A_2 be the vertices Q and R respectively, and let B_1 be the foot of the perpendicular from P on QR.

The resulting fundamental equations are, setting $p = \frac{n}{d}$:

$$q\alpha_1 = r\alpha_2 = \pi,$$

$$n\gamma_1 + n\gamma_2 = \pi d.$$

By reflecting PQR repeatedly in its sides, we get the sequences of vertices $A_1A_2A_3\cdots$ and $B_1B_2B_3\cdots$,

which repeat themselves after $2n$ terms.

The resulting polyhedron is denoted by the Wythoff symbol $p|q\ r$. Its vertex configuration is $(q.r.q.r.\cdots.q.r)$ ($2n$ terms), and its vertex density is d. The vertex figure and the dual prototile are $2n$-gons.

4.2. C **is at the intersection of the side** PQ **with bisector of the opposite angle** R**.**

Let A_1, A_2 and A_3 be the vertices Q, R and P, and let B_1 and B_2 be the feet of the perpendiculars from C on QR and RP, respectively.

The resulting fundamental equations are:

$$q\alpha_1 = 2r\alpha_2 = p\alpha_3 = \pi,$$

$$\gamma_1 + 2\gamma_2 + \gamma_3 = \pi.$$

By reflecting A_2, B_1 and B_2 in QR, we get the images A_4, B_4 and B_3, respectively.

The resulting polyhedron is denoted by the Wythoff symbol $p\ q|r$, and its vertex configuration is $(p.2r.q.2r)$. The vertex figure and the dual prototile are quadrilaterals.

4.3. C **is at the incenter of** PQR**.**

Let A_1, A_2 and A_3 be the vertices P, Q and R, and let B_1, B_2 and B_3 be the feet of the perpendiculars from C on PQ, QR and RP, respectively.

The resulting fundamental equations are:

$$2p\alpha_1 = 2q\alpha_2 = 2r\alpha_3 = \pi,$$

$$\gamma_1 + \gamma_2 + \gamma_3 = \pi.$$

The resulting polyhedron is denoted by the Wythoff symbol $p\ q\ r|$, and its vertex configuration is $(2p.2q.2r)$. The vertex figure and the dual prototile are triangles.

4.4. C **traces a snub polyhedron.**

In the previous positions, the symmetry group of the polyhedron is generated by reflections. In particular, the polyhedron is reflexible. We now discuss a fourth position, which usually traces a chiral polyhedron, i.e., a polyhedron with a symmetry group which consists of rotations only[3]. This is done by considering only images under an even number of reflections (as was done for the dihedral kaleidoscope). In this case, it is easier to study the dual tiling directly, and to infer the existence of C without an actual construction.

Let O be the *Fermat* point of the Schwarz triangle PQR, i.e, the point where the sides subtend equal angles (assuming it exists[4]). Reflect O in the sides and get an hexagon $A_1A_2\cdots A_6$ with angles $\frac{2\pi}{3}$, $\frac{2\pi}{p}$, $\frac{2\pi}{3}$, $\frac{2\pi}{q}$, $\frac{2\pi}{3}$ and $\frac{2\pi}{r}$ respectively, where odd indices refer to the images of O, and even indices refer to the vertices P, Q and R. Reflecting this hexagon any even number of times, we get an isohedral, vertically regular tiling of the sphere, i.e., the dual of a uniform tiling. The latter consists of a $\{p\}$, a $\{q\}$ and a $\{r\}$ with centers at P, Q and R, respectively, alternating with three, so-called *snub*, $\{3\}$'s. Let C be the common vertex of these six polygons (since the snub $\{3\}$'s are congruent, it is located at the circumcenter of $A_1A_3A_5$), and let B_i, for $i = 1, 2, \cdots, 6$, be the foot of the perpendicular from C to A_iA_{i+1}.

The resulting fundamental equations are:

$$3\alpha_1 = p\alpha_2 = q\alpha_4 = r\alpha_6 = \pi,$$

[3] However, (5/2 3 3) and (3/2 3/2 5/2) being isosceles, they yield reflexible snub polyhedra.

[4] The existence of O is verified by a continuity argument, at least for the case where all the angles of PQR are smaller then $2\pi/3$ (this is not the case for (3/2 3/2 5/2) and (3/2 5/3 2)).

$$3\gamma_1 + \gamma_2 + \gamma_4 + \gamma_6 = \pi.$$

Here, we counted one snub $\{3\}$ thrice, because the snub $\{3\}$s are all congruent. The resulting *snub* polyhedron is denoted by the Wythoff symbol $|p\ q\ r$, and its vertex configuration is $(3.\ p.\ 3.\ q.\ 3.\ r)$. The vertex figure and the dual prototile are hexagons.

Note that in all the cases, the occurrence of $\alpha = \frac{\pi}{2}$ implies that the corresponding tile is a $\{2\}$, i.e., a digon, and may be discarded.

5. Exceptional Polyhedra.

An polyhedron is *orientable* if its faces may be coherently oriented, that is, assigned orientations in such a way that the orientations induced on an edge common to two faces are opposite. It is easy to verify, that the Wythoff construction always yields orientable polyhedra, assuming that vertices which belong to nonadjacent Schwarz triangles are considered distinct, even if they coincide. The number of the polyhedron vertices may be readily found by dividing the order of the kaleidoscope symmetry group by the number of copies of adjacent Schwarz triangles which share a vertex, i. e., by two for $p\ q|r$ or $|p\ q\ r$, and by n for $\frac{n}{d}\,|q\ r$.

We will now discuss two particular cases where the Wythoff construction yields only pairs of coinciding vertices, that, when identified, are the vertices of a nonorientable, or *one-sided*, polyhedron. In these cases, the number of real vertices will be of course only a half of the expected number. The discussion is based on the phenomenon, described in section 4, that a point object on the bisector of a dihedral kaleidoscope with angle $\frac{\pi}{q}$, q rational with an even denominator, yields a double $\{2q\}$.

For conclusion, we shall have a brief, independent discussion about the solution for the only non-Wythoffian polyhedron in existence.

5.1. Polyhedra $p\ q\ r|$ with an even denominator.

Consider a Schwarz triangle PQR, with an angle $\frac{\pi}{r}$ at R, r rational with an even denominator. Suppose the point object C is located in the incenter of PQR. In particular, it lies on the bisector at R. As we have seen, the images of C trace a $\{2p\}$, a $\{2q\}$ and a $\{2r\}$, with centers at P, Q and R, respectively. However, since r has an even denominator, we find that the face with center at R, which is traced by reflections at RP and RQ only, is a double $\{2r\}$. When transversing it once, PQR is reflected in the bisector at R, and the faces with centers at P and Q are reflected into two similar faces with centers at the images of P and Q. Thus, in addition to the double $\{2r\}$, we have at C two $\{p\}$'s and two $\{q\}$'s, arranged in the cyclic order $(2r.\ p.\ q.\ 2r.\ q.\ p)$. By discarding the double $\{2r\}$'s, we get a single, one-sided polyhedron. The nonorientability is due to orientation reversal: Trying to find a coherent orientation on the faces and considering the four faces incident at a vertex, we notice that two of them has to be retrograde, i.e., the vertex configuration is $(p.\ q.\ p'.\ q')$. However, when considering the faces adjacent to a discarded double $\{2r\}$, none of the four faces incident at a vertex may be retrograde.

It is interesting to note, that the enumeration of the faces at C does not define the polyhedron well, and the direct algorithmic approach in section 3 fails. However, by taking the $\{2r\}$'s into account, and solving the equations set in section 4.3, the metrical properties of these exceptional polyhedra may be still computed.

The Euler characteristic can be obtained from the basic value discussed in section 4: By considering the fundamental triangulation and removing the double $\{2r\}$'s, the balance of edges and faces doesn't change, and the number of vertices is reduced by V_r (see section 4). Thus, we get for this case

$$\chi = \frac{g}{2}\left(\frac{1}{n_p} + \frac{1}{n_q} - 1\right).$$

The density is not-well define, as these polyhedra do not produce an even covering of the sphere.

5.2. Hemi polyhedra $p\ p'|r$**.**

Consider a Schwarz triangle *PQR*, where the angles $\frac{\pi}{p}$ and $\frac{\pi}{q}$ are complementary, and assume that $q = p' < 2 < p$. Reflecting the side *PR* in *PQ*, we get an arc which meets the extension of *RQ* beyond *Q* at a point *S*. It is clear that the sides of the spherical triangle *PSR* are all arcs of symmetry of the group generated by *PQR*, and thus it is itself a Schwarz triangle, say $(\frac{p}{2}\ s\ r)$, where *s* is a rational greater than one. It follows that the incenter *C* of *PSR* is also the point where the side *PQ* of *PQR* meets the bisector of the opposite angle. Thus, considering the polyhedra traced by the images of *C*, we find that the polyhedra $p\ p'|r$ and $\frac{p}{2}\ s\ r|$ have the same vertices. Of course, the vertex configurations are different: $(p.2r.p'.2r)$ for the former, $(p.2s.2r)$ for the latter. However, if *s* has an even denominator, the double $\{2s\}$'s in $\frac{p}{2}\ s\ r|$ may discarded as above, and we are left with the vertex configuration $(p.2r.p'.2r)$, that is $p\ p'|r$. The last term of the vertex configuration may be written as $2r$ rather than $(2r)'$, because the {2r}'s are great circles, and thus the same orientation can be designated either retrograde or not. This property of the $\{2r\}$'s follows from the observation that *C* is the incenter of the lune obtained by extending *RP* and *RQ* beyond *P* and *Q*. The property that such polyhedra possess equatorial faces which separate them in half justifies labeling them *hemi*.

It is interesting to note, that if *s* has an even denominator, than *CPS* is the Schwarz triangle $(2\ p\ 2s)$ (or, the hemi polyhedron share the vertices with $2|p\ 2s$), where $2s$ has an odd numerator. However, it may be shown that the only Schwarz triangle $(2\ p\ q)$ with *q* rational, greater than two, and with an even numerator is (2 3 4). Thus, it follows that the only hemi polyhedron which is orientable is $3\ \frac{3}{2}|3$ (cf. [CLM], p. 417).

In contrast to the previous case, it is easy to check that the metrical properties of the polyhedron $p\ p'|r$ are computable from its vertex configuration, once we write it $(p.2r.p'.2r)$ rather than $(p.2r.p'.(2r)')$. In fact, just one step of the algorithm yields the exact result. The geometric reason behind this contrast is related to the vertex figure of the two types of nonorientable polyhedra (cf. [CLM], p. 417 and 419): The vertex figure of a general $pqr|$ is a crossed parallelogram, which is not determined given its sides and its inscribability in a circle. However, the vertex figure of $p\ p'|r$ is a crossed rectangle, and the extra information that the crossed sides pass through the center of the circle does determine the vertex figure.

As the Wythoff construction generates an orientable two sided covering of $p\ p'|r$, its Euler characteristic is half of the basic one, that is

$$\chi = \frac{g}{4}\left(\frac{2}{n_p} + \frac{1}{n_r} - 1\right).$$

5.3. The last polyhedron $|3\ \frac{5}{2}\ \frac{3}{2}\ \frac{5}{3}$**.**

The only uniform polyhedron which has more than six faces at a vertex, and the only one which cannot be constructed by the Wythoff construction (or a minute modification of it), has the vertex configuration $(4.\frac{5}{2}.4.3.4.\frac{5}{3}.4.\frac{3}{2})$. Again, the enumeration of faces incident at a vertex does not determine the polyhedron, and therefore a direct use of the uniform solution fails. However, by considering the Schwarz triangle $(3\ \frac{5}{2}\ \frac{5}{3})$ and its reflection in the perpendicular bisector of its shortest side (which is an arc of symmetry of the generated group), it may be shown (cf. [CLM], section 11), that the oppositely oriented pairs of triangles and pentagrams of $|3\ \frac{5}{2}\ \frac{3}{2}\ \frac{5}{3}$ also belong to an enantiomorphous and vertex sharing pair of $|3\ \frac{5}{2}\ \frac{5}{3}$'s. Actually, both pentagrams belong to both snub polyhedra, with roles interchanged, and each triangle is a non-snub triangle of one of the pair. We can conclude easily that the last uniform polyhedron is a second instance of an orientable hemi polyhedron. Furthermore, solving the snub polyhedra as in section 4.4, we can complete the solution by computing the triangulation of the extra squares using the fundamental equation (3), section 2. The Euler characteristic has the bizarre value of $\chi = -56$, computable from the actual counts of vertices, edges and faces.

6. References.

[BC] Ball, W. W. R & Coxeter, H. S. M., *Mathematical Recreations and Essays*, Thirteenth Edition, Dover, New York, 1987.

[C] Coxeter, H. S. M., *Regular Polytopes*, Third Edition, Dover, New York, 1973.

[CLM] Coxeter, H. S. M., Longuet-Higgins, M. S. & Miller, J. C. P., *Uniform Polyhedra*, Phil. Trans. Royal Soc. London, Ser. A, 246 (1953), 401-409.

[CR] Cundy, H. M. & Rollett, A. P., *Mathematical Models*, Third Edition, Tarquin, Stradbroke, 1981.

[GMS] Grünbaum, B., Miller, J. C. P. & Shephard, G. C., *Uniform Tilings with Hollow Tiles*, in *The Geometric Vein - The Coxeter Festschrift*, C. Davis et al., eds., Springer-Verlag, New York, 1982, 17-64.

[GS] Grübaum, B. & Shephard, G. C., *Tilings and Patterns*, Freeman, New York, 1987.

[Ha] Har'El, Z., *Kaleido - Kaleidoscopic Construction of Uniform Polyhedra*, Department of Mathematics, Technion, Haifa, 1992.

[Hm] Hume, A., *Exact Descriptions of Regular and Semi-regular Polyhedra and Their Duals*, Computing Science Technical Report No. 130, AT&T Bell Laboratories, Murray Hill, 1986.

[Hy] Huybers, P., *Uniform Polyhedra for Building Structures*, Bull. Inter. Assos. Shells and Spatial Structures, 21 (1980), 27-38.

[J] Johnson, N. W., *Convex Polyhedra with Regular Faces*, Canad. J. Math., 18 (1966), 169-200.

[L] Lines, L., *Solid Geometry*, Dover, New York, 1961.

[M] Moritz, R., *On Napier's Fundamental Theorem Relating to Right Spherical Triangles*, Amer. Math. Monthly, 22 (1915), 220-222.

[S] Skilling, J., *The Complete Set of Uniform Polyhedra*, Phil. Trans. Royal Soc. London, Ser. A, 278 (1975), 111-135.

[W1] Wenninger, M. J., *Polyhedron Models*, Cambridge University Press, Cambridge, 1971.

[W2] Wenninger, M. J., *Dual Models*, Cambridge University Press, Cambridge, 1984.

Appendix I: Schwarz Triangles.

To facilitate the enumeration of Schwarz triangles, one notices that for the covering to be simple, $(p\ q\ r)$ must be a *Möbius triangle*, that is, one of the triangles $D_{1/n} = (2\ 2\ n)$ (with $n = 2, 3, \cdots$), $T_1 = (2\ 3\ 3)$, $O_1 = (2\ 3\ 4)$ and $I_1 = (2\ 3\ 5)$, which are the fundamental domains of the full dihedral, tetrahedral, octahedral and icosahedral symmetry groups, respectively. A Schwarz triangle which produces a d-fold covering of the sphere can be decomposed to d copies of one of the Möbius triangles. These properties may be used to synthesize Schwarz triangles, as we now explain.

Let

$$S_1 = (p\ x\ r_1\ ;\ y\ v\ w_1)$$

and

$$S_2 = (x'\ q\ r_2\ ;\ u\ y\ w_2)$$

be two Schwarz triangles (where we included in the symbol also the sides opposite the respective angles), which have a common edge y and complementary angles $\frac{\pi}{x}$ and $\frac{\pi}{x'}$. Then, S_1 and S_2 can be pasted along the common edge, and produce a new triangle

$$S_1 + S_2 = (p\ q\ r\ ;\ u\ v\ w),$$

where we have set

$$\frac{1}{r} = \frac{1}{r_1} + \frac{1}{r_2},$$

$$w = w_1 + w_2.$$

This is a Schwarz triangle if $r > 1$. As usual, $2S$ is a shorthand for $S + S$.

In few cases, S_1 and S_2 can be pasted together in more then one way, to produce several different Schwarz triangles. In particular, if S_1 and S_2 are two copies of the same right-angled triangle $(p\ q\ 2\ ;\ u\ v\ w)$, with $p, q > 2$ and $p \neq q$, they can be pasted along each of the legs, to produce two isosceles triangles, with the same area but different perimeter, namely $(q\ q\ \frac{p}{2}\ ;\ w\ w\ 2u)$ and $(p\ p\ \frac{q}{2}\ ;\ w\ w\ 2v)$.

Starting from the Möbius triangles we get the denumerable family of dihedral Schwarz triangles $D_{d/n} = (2\ 2\ \frac{n}{d})$ (with $d = 1, \cdots, n-1$), and the tetrahedral, octahedral and icosahedral triangles listed in tables 1 through 3. The triangles are arranged by increasing area: The area of I_d, for instance, is d times the area of I_1. In the cases where there are several triangles with the same area, they are ordered by increasing perimeter and distinguished from one another by a letter, e.g., I_{2a} and I_{2b}. The sides are given in terms of the legs s, u and v of T_1 and I_1[5]. Because of space considerations, we list just one of the several ways to split each Schwarz triangle into smaller ones. It is interesting that every triangle (except the smallest) can always be split into two triangular pieces, with only one exception: The the trirectangular triangle $D_{1/2}$, if considered as an icosaheral Schwarz triangle, can only be split into four pieces or more. The listed splitting is the symmetric one: An equilateral triangle, $(\frac{5}{2}\ \frac{5}{2}\ \frac{5}{2})$, surrounded by three copies of its half, the right-angled triangle $(5\ \frac{5}{2}\ 2)$. Triangles which belong to a proper symmetry subgroup are flagged.

[5] It may be shown that $\cos 2s = -\frac{1}{3}$, $\cos 2u = \frac{\sqrt{5}}{3}$ and $\cos 2v = \frac{\sqrt{5}}{5}$.

Table 1: Tetrahedral Schwarz Triangles					
	symbol	sides			splitting
T_1	(3 3 2)	s	s	$\pi-2s$	
T_2	(3 3 $\frac{3}{2}$)	$\pi-2s$	$\pi-2s$	$2s$	$2T_1$
T_3	(3 2 $\frac{3}{2}$)	s	$2s$	$\pi-s$	T_1+T_2
T_5	(2 $\frac{3}{2}$ $\frac{3}{2}$)	$\pi-2s$	$\pi-s$	$\pi-s$	T_2+T_3
T_6	($\frac{3}{2}$ $\frac{3}{2}$ $\frac{3}{2}$)	$2s$	$2s$	$2s$	$2T_3$

Table 2: Octahedral Schwarz Triangles						
	symbol	sides			splitting	
O_1	(4 3 2)	$\frac{\pi}{2}-s$	$\frac{\pi}{4}$	s		
O_{2a}	(3 3 2)	s	s	$\pi-2s$	$2O_1$	T_1
O_{2b}	(4 4 $\frac{3}{2}$)	s	s	$\frac{\pi}{2}$	$2O_1$	
O_3	(4 2 2)	$\frac{\pi}{4}$	$\frac{\pi}{2}$	$\frac{\pi}{2}$	O_1+O_{2a}	$D_{1/4}$
O_{4a}	(3 3 $\frac{3}{2}$)	$\pi-2s$	$\pi-2s$	$2s$	$2O_{2a}$	T_2
O_{4b}	(4 3 $\frac{4}{3}$)	s	$\frac{\pi}{2}$	$\pi-s$	$O_{2a}+O_{2b}$	
O_5	(4 2 $\frac{3}{2}$)	$\frac{\pi}{2}-s$	$\pi-s$	$\frac{3\pi}{4}$	O_1+O_{4b}	
O_{6a}	(2 2 2)	$\frac{\pi}{2}$	$\frac{\pi}{2}$	$\frac{\pi}{2}$	$2O_3$	$D_{1/2}$
O_{6b}	(3 2 $\frac{3}{2}$)	s	$2s$	$\pi-s$	$O_{2a}+O_{4a}$	T_3
O_7	(3 2 $\frac{4}{3}$)	$\frac{\pi}{4}$	$\pi-s$	$\frac{\pi}{2}+s$	O_3+O_{4b}	
O_9	(2 2 $\frac{4}{3}$)	$\frac{\pi}{2}$	$\frac{\pi}{2}$	$\frac{3\pi}{4}$	$O_{4b}+O_5$	$D_{3/4}$
O_{10}	(2 $\frac{3}{2}$ $\frac{3}{2}$)	$\pi-2s$	$\pi-s$	$\pi-s$	$2O_5$	T_5
O_{11}	(2 $\frac{3}{2}$ $\frac{4}{3}$)	s	$\frac{3\pi}{4}$	$\frac{\pi}{2}+s$	$O_{6b}+O_5$	
O_{12}	($\frac{3}{2}$ $\frac{3}{2}$ $\frac{3}{2}$)	$2s$	$2s$	$2s$	$2O_{6b}$	T_6
O_{14}	($\frac{3}{2}$ $\frac{4}{3}$ $\frac{4}{3}$)	$\frac{\pi}{2}$	$\pi-s$	$\pi-s$	$2O_7$	

Table 3: Icosahedral Schwarz Triangles						
	symbol	sides			splitting	
I_1	$(5\ 3\ 2)$	u	v	$\frac{\pi}{2}-u-v$		
I_{2a}	$(3\ 3\ \frac{5}{2})$	$\frac{\pi}{2}-u-v$	$\frac{\pi}{2}-u-v$	$2u$	$2I_1$	
I_{2b}	$(5\ 5\ \frac{3}{2})$	$\frac{\pi}{2}-u-v$	$\frac{\pi}{2}-u-v$	$2v$	$2I_1$	
I_3	$(5\ \frac{5}{2}\ 2)$	v	$\frac{\pi}{2}-v$	$2v$	I_1+I_{2b}	
I_4	$(5\ 3\ \frac{5}{3})$	$\frac{\pi}{2}-u-v$	$2v$	$\frac{\pi}{2}+u-v$	$I_{2a}+I_{2b}$	
I_{6a}	$(\frac{5}{2}\ \frac{5}{2}\ \frac{5}{2})$	$2v$	$2v$	$2v$	$2I_3$	
I_{6b}	$(5\ 3\ \frac{3}{2})$	$2u$	$\frac{\pi}{2}+u-v$	$\frac{\pi}{2}-u+v$	$I_{2a}+I_4$	
I_{6c}	$(5\ 5\ \frac{5}{4})$	$2v$	$2v$	$\pi-2v$	$2I_3$	
I_7	$(3\ \frac{5}{2}\ 2)$	$\frac{\pi}{2}-v$	$\frac{\pi}{2}-u$	$\frac{\pi}{2}+u-v$	I_3+I_4	
I_8	$(5\ \frac{5}{2}\ \frac{3}{2})$	$\frac{\pi}{2}-u-v$	$\frac{\pi}{2}-u+v$	$\pi-2v$	$I_{2a}+I_{6b}$	
I_9	$(5\ 2\ \frac{5}{3})$	v	$\pi-2v$	$\frac{\pi}{2}+v$	I_3+I_{6c}	
I_{10a}	$(3\ \frac{5}{2}\ \frac{5}{3})$	$2v$	$\frac{\pi}{2}+u-v$	$\frac{\pi}{2}-u+v$	I_4+I_{6a}	
I_{10b}	$(5\ 3\ \frac{5}{4})$	$\frac{\pi}{2}-u-v$	$\pi-2v$	$\frac{\pi}{2}+u+v$	I_4+I_{6c}	
I_{11}	$(5\ 2\ \frac{3}{2})$	u	$\frac{\pi}{2}+u+v$	$\pi-v$	I_1+I_{10b}	
I_{13}	$(3\ 2\ \frac{5}{3})$	$\frac{\pi}{2}-v$	$\frac{\pi}{2}-u+v$	$\frac{\pi}{2}+u$	$I_{6b}+I_7$	
I_{14a}	$(\frac{5}{2}\ \frac{5}{2}\ \frac{3}{2})$	$\frac{\pi}{2}+u-v$	$\frac{\pi}{2}+u-v$	$\pi-2v$	$2I_7$	
I_{14b}	$(3\ 3\ \frac{5}{4})$	$\frac{\pi}{2}+u-v$	$\frac{\pi}{2}+u-v$	$\pi-2u$	$2I_7$	
I_{15}	$(2\ 2\ 2)$	$\frac{\pi}{2}$	$\frac{\pi}{2}$	$\frac{\pi}{2}$	$I_{6a}+3I_3$	$D_{1/2}$
I_{16}	$(3\ \frac{5}{2}\ \frac{5}{4})$	$2v$	$\frac{\pi}{2}-u+v$	$\frac{\pi}{2}+u+v$	$I_{6a}+I_{10a}$	
I_{17}	$(\frac{5}{2}\ 2\ \frac{3}{2})$	$\frac{\pi}{2}-u$	$\frac{\pi}{2}-u+v$	$\frac{\pi}{2}+v$	I_8+I_9	
I_{18a}	$(\frac{5}{2}\ \frac{5}{3}\ \frac{5}{3})$	$2v$	$\pi-2v$	$\pi-2v$	$2I_9$	
I_{18b}	$(3\ \frac{5}{3}\ \frac{3}{2})$	$\frac{\pi}{2}-u-v$	$\pi-2u$	$\frac{\pi}{2}+u+v$	I_8+I_{10b}	
I_{19}	$(3\ 2\ \frac{5}{4})$	v	$\frac{\pi}{2}+u+v$	$\pi-u$	I_9+I_{10b}	
I_{21}	$(\frac{5}{2}\ 2\ \frac{5}{4})$	$\frac{\pi}{2}-v$	$\pi-2v$	$\pi-v$	$I_{10b}+I_{11}$	
I_{22}	$(\frac{5}{2}\ \frac{3}{2}\ \frac{3}{2})$	$2u$	$\frac{\pi}{2}+u+v$	$\frac{\pi}{2}+u+v$	$2I_{11}$	
I_{23}	$(2\ \frac{5}{3}\ \frac{3}{2})$	$\frac{\pi}{2}+u-v$	$\frac{\pi}{2}+u$	$\frac{\pi}{2}+v$	$I_{10a}+I_{13}$	
I_{26}	$(\frac{5}{3}\ \frac{5}{3}\ \frac{3}{2})$	$\frac{\pi}{2}-u+v$	$\frac{\pi}{2}-u+v$	$\pi-2v$	$2I_{13}$	
I_{27}	$(2\ \frac{5}{3}\ \frac{5}{4})$	$2v$	$\frac{\pi}{2}+v$	$\pi-v$	$I_{11}+I_{16}$	
I_{29}	$(2\ \frac{5}{2}\ \frac{5}{4})$	$\frac{\pi}{2}-u-v$	$\pi-v$	$\pi-u$	$I_{11}+I_{18b}$	
I_{32}	$(\frac{5}{3}\ \frac{3}{2}\ \frac{5}{4})$	$\frac{\pi}{2}+u-v$	$\pi-2v$	$\frac{\pi}{2}+u+v$	$I_{14a}+I_{18a}$	
I_{34}	$(\frac{3}{2}\ \frac{3}{2}\ \frac{5}{4})$	$\frac{\pi}{2}-u+v$	$\frac{\pi}{2}-u+v$	$\pi-2u$	$2I_{17}$	
I_{38}	$(\frac{3}{2}\ \frac{5}{4}\ \frac{5}{4})$	$2v$	$\frac{\pi}{2}+u+v$	$\frac{\pi}{2}+u+v$	$2I_{19}$	
I_{42}	$(\frac{5}{4}\ \frac{5}{4}\ \frac{5}{4})$	$\pi-2v$	$\pi-2v$	$\pi-2v$	$2I_{21}$	

Appendix II: Uniform Polyhedra

In tables 4 to 8, we list the seventy-five nondihedral uniform polyhedra, as well as the five pentagonal prisms and antiprisms, grouped by generating Schwarz triangles. For each polyhedron we indicate a figure number in this appendix, its Wythoff and vertex configuration symbols, and the values of its Euler characteristic χ and density D (if well-defined). Nonorientable polyhedra are marked by starring their characteristic. For reference, we indicate for each polyhedron a figure number in [CLM], pp. 439-448, and a model number in [W1]. The polyhedron names listed in tables 5 to 8 are taken from [W2], where they are attributed to Norman W. Johnson, but note they sometimes vary among authors. Our figures represent wireframe images of the listed uniform polyhedra and their duals (the latter are indicated by a starred figure number[6]). Although the figures are two dimensional, depth is faithfully represented by the variable thickness of the wires. The drawings were made using the UNIX[7] utility *pic*, from directives generated by *kaleido* (cf. [Ha]).

Table 4: Dihedral Uniform Polyhedra

	fig	symbol		name *dual*	χ	D
$D_{1/5}$	1	2 5|2	(4. 4. 5)	pentagonal prism *pentagonal dipyramid*	2	1
	2	|2 2 5	(3. 3. 3. 5)	pentagonal antiprism *pentagonal deltohedron*	2	1
$D_{2/5}$	3	$2\ \frac{5}{2}\ \|2$	$(4.\ 4.\ \frac{5}{2})$	pentagrammic prism *pentagrammic dipyramid*	2	2
	4	$\|2\ 2\ \frac{5}{2}$	$(3.\ 3.\ 3.\ \frac{5}{2})$	pentagrammic antiprism *pentagrammic deltohedron*	2	2
$D_{3/5}$	5	$\|2\ 2\ \frac{5}{3}$	$(3.\ 3.\ 3.\ \frac{5}{3})$	pentagrammic crossed antiprism *pentagrammic concave deltohedron*	2	3

Table 5: Tetrahedral Uniform Polyhedra

	fig	symbol		name *dual*	χ	D	ref
T_1	6	3|2 3	(3. 3. 3)	tetrahedron *tetrahedron*	2	1	15,1
	7	2 3|3	(6. 6. 3)	truncated tetrahedron *triakistetrahedron*	2	1	16,6
T_2	8	$\frac{3}{2}\ 3\|3$	$(6.\ \frac{3}{2}\ .\ 6.\ 3)$	octahemioctahedron *octahemioctacron*	0		37,68
T_3	9	$\frac{3}{2}\ 3\|2$	$(4.\ \frac{3}{2}\ .\ 4.\ 3)$	tetrahemihexahedron *tetrahemihexacron*	1*		36,67

[6] The ten unbounded polyhedra in figures 8*,9*,20*,54*,56*,66*,68*,75*,76*,80* are different from their [W2] counterparts. They use the *more correctly shown* faces of [W2], p. 103.

[7] UNIX is a trademark of AT&T Bell Laboratories.

Table 6: Octahedral Uniform Polyhedra							
	fig	symbol		name *dual*	χ	D	ref
O_1	10	4|2 3	(3. 3. 3. 3)	octahedron *cube*	2	1	17,2
	11	3|2 4	(4. 4. 4)	cube *octahedron*	2	1	18,3
	12	2|3 4	(3. 4. 3. 4)	cuboctahedron *rhombic dodecahedron*	2	1	19,11
	13	2 4|3	(6. 6. 4)	truncated octahedron *tetrakishexahedron*	2	1	20,7
	14	2 3|4	(8. 8. 3)	truncated cube *triakisoctahedron*	2	1	21,8
	15	3 4|2	(4. 3. 4. 4)	rhombicuboctahedron *deltoidal icositetrahedron*	2	1	22,13
	16	2 3 4|	(4. 6. 8)	truncated cuboctahedron *disdyakisdodecahedron*	2	1	23,15
	17	|2 3 4	(3. 3. 3. 3. 4)	snub cube *pentagonal icositetrahedron*	2	1	24,17
O_{2b}	18	$\frac{3}{2}$ 4|4	(8. $\frac{3}{2}$. 8. 4)	small cubicuboctahedron *small hexacronic icositetrahedron*	−4	2	38,69
O_4	19	3 4| $\frac{4}{3}$	($\frac{8}{3}$. 3. $\frac{8}{3}$. 4)	great cubicuboctahedron *great hexacronic icositetrahedron*	−4	4	50,77
	20	$\frac{4}{3}$ 4|3	(6. $\frac{4}{3}$. 6. 4)	cubohemioctahedron *hexahemioctacron*	−2*		51,78
	21	$\frac{4}{3}$ 3 4|	($\frac{8}{3}$. 6. 8)	cubitruncated cuboctahedron *tetradyakishexahedron*	−4	4	52,79
O_5	22	$\frac{3}{2}$ 4|2	(4. $\frac{3}{2}$. 4. 4)	great rhombicuboctahedron *great deltoidal icositetrahedron*	2	5	59,85
	23	$\frac{3}{2}$ 2 4|	(8. 4. $\frac{8}{7}$. $\frac{4}{3}$)	small rhombihexahedron *small rhombihexacron*	−6*		60,86
O_7	24	2 3| $\frac{4}{3}$	($\frac{8}{3}$. $\frac{8}{3}$. 3)	stellated truncated hexahedron *great triakisoctahedron*	2	7	66,92
	25	$\frac{4}{3}$ 2 3|	($\frac{8}{3}$. 4. 6)	great truncated cuboctahedron *great disdyakisdodecahedron*	2	1	67,93
O_{11}	26	$\frac{4}{3}$ $\frac{3}{2}$ 2|	(4. $\frac{8}{3}$. $\frac{4}{3}$. $\frac{8}{5}$)	great rhombihexahedron *great rhombihexacron*	−6*		82,103

Table 7: Icosahedral Uniform Polyhedra							
	fig	symbol		name *dual*	χ	D	ref
I_1	27	5|2 3	(3. 3. 3. 3. 3)	icosahedron *dodecahedron*	2	1	25,4
	28	3|2 5	(5. 5. 5)	dodecahedron *icosahedron*	2	1	26,5
	29	2|3 5	(3. 5. 3. 5)	icosidodecahedron *rhombic triacontahedron*	2	1	28,12
	30	2 5|3	(6. 6. 5)	truncated icosahedron *pentakisdodecahedron*	2	1	27,9
	31	2 3|5	(10. 10. 3)	truncated dodecahedron *triakisicosahedron*	2	1	29,10
	32	3 5|2	(4. 3. 4. 5)	rhombicosidodecahedron *deltoidal hexecontahedron*	2	1	30,14
	33	2 3 5|	(4. 6. 10)	truncated icosidodechedon *disdyakistriacontahedron*	2	1	31,16
	34	|2 3 5	(3. 3. 3. 3. 5)	snub dodecahedron *pentagonal hexecontahedron*	2	1	32,18
I_{2a}	35	$3\|\frac{5}{2}$ 3	$(\frac{5}{2}.3.\frac{5}{2}.3.\frac{5}{2}.3)$	small ditrigonal icosidodecahedron *small triambic icosahedron*	−8	2	39,70
	36	$\frac{5}{2}$ 3|3	$(6.\frac{5}{2}.6.3)$	small icosicosidodecahedron *small icosacronic hexecontahedron*	−8	2	40,71
	37	$\|\frac{5}{2}$ 3 3	$(3.\frac{5}{2}.3.3.3.3)$	small snub icosicosidodecahedron *small hexagonal hexecontahedron*	−8	2	41,110
I_{2b}	38	$\frac{3}{2}$ 5|5	$(10.\frac{3}{2}.10.5)$	small dodecicosidodecahedron *small dodecacronic hexecontahedron*	−16	2	42,72
I_3	39	5|2 $\frac{5}{2}$	$(\frac{5}{2}.\frac{5}{2}.\frac{5}{2}.\frac{5}{2}.\frac{5}{2})$	small stellated dodecahedron *great dodecahedron*	−6	3	43,20
	40	$\frac{5}{2}$ |2 5	(5. 5. 5. 5. 5)/2	great dodecahedron *small stellated dodecahedron*	−6	3	44,21
	41	$2\|\frac{5}{2}$ 5	$(\frac{5}{2}.5.\frac{5}{2}.5)$	dodecadodecahedron *medial rhombic triacontahedron*	−6	3	45,73
	42	2 $\frac{5}{2}$ |5	$(10.10.\frac{5}{2})$	truncated great dodecahedron *small stellapentakisdodecahedron*	−6	3	47,75
	43	$\frac{5}{2}$ 5|2	$(4.\frac{5}{2}.4.5)$	rhombidodecadodecahedron *medial deltoidal hexecontahedron*	−6	3	48,76
	44	2 $\frac{5}{2}$ 5|	$(10.4.\frac{10}{9}.\frac{4}{3})$	small rhombidodecahedron *small rhombidodecacron*	−18*		46,74
	45	|2 $\frac{5}{2}$ 5	$(3.3.\frac{5}{2}.3.5)$	snub dodecadodecahedron *medial pentagonal hexecontahedron*	−6	3	49,111

Table 7: Icosahedral Uniform Polyhedra							
	fig	symbol		name *dual*	χ	D	ref
I_4	46	$3\|\frac{5}{3}\ 5$	$(\frac{5}{3}.5.\frac{5}{3}.5.\frac{5}{3}.5)$	ditrigonal dodecadodecahedron *medial triambic icosahedron*	−16	4	53,80
	47	$3\ 5\|\frac{5}{3}$	$(\frac{10}{3}.3.\frac{10}{3}.5)$	great ditrigonal dodecicosidodecahedron *great ditrigonal dodecacronic hexecontahedron*	−16	4	54,81
	48	$\frac{5}{3}\ 3\|5$	$(10.\frac{5}{3}.10.3)$	small ditrigonal dodecicosidodecahedron *small ditrigonal dodecacronic hexecontahedron*	−16	4	55,82
	49	$\frac{5}{3}\ 5\|3$	$(6.\frac{5}{3}.6.5)$	icosidodecadodecahedron *medial icosacronic hexecontahedron*	−16	4	56,83
	50	$\frac{5}{3}\ 3\ 5\|$	$(\frac{10}{3}.6.10)$	icositruncated dodecadodecahedron *tridyakisicosahedron*	−16	4	57,84
	51	$\|\frac{5}{3}\ 3\ 5$	$(3.\frac{5}{3}.3.3.3.5)$	snub icosidodecadodecahedron *medial hexagonal hexecontahedron*	−16	4	58,112
I_{6b}	52	$\frac{3}{2}\|3\ 5$	$(3.5.3.5.3.5)/2$	great ditrigonal icosidodecahedron *great triambic icosahedron*	−8	6	61,87
	53	$\frac{3}{2}\ 5\|3$	$(6.\frac{3}{2}.6.5)$	great icosicosidodecahedron *great icosacronic hexecontahedron*	−8	6	62,88
	54	$\frac{3}{2}\ 3\|5$	$(10.\frac{3}{2}.10.3)$	small icosihemidodecahedron *small icosihemidodecacron*	−4*		63,89
	55	$\frac{3}{2}\ 3\ 5\|$	$(10.6.\frac{10}{9}.\frac{6}{5})$	small dodecicosahedron *small dodecicosacron*	−28*		64,90
I_{6c}	56	$\frac{5}{4}\ 5\|5$	$(10.\frac{5}{4}.10.5)$	small dodecahemidodecahedron *small dodecahemidodecacron*	−12*		65,91
I_7	57	$3\|2\ \frac{5}{2}$	$(\frac{5}{2}.\frac{5}{2}.\frac{5}{2})$	great stellated dodecahedron *great icosahedron*	2	7	68,22
	58	$\frac{5}{2}\|2\ 3$	$(3.3.3.3.3)/2$	great icosahedron *great stellated dodecahedron*	2	7	69,41
	59	$2\|\frac{5}{2}\ 3$	$(\frac{5}{2}.3.\frac{5}{2}.3)$	great icosidodecahedron *great rhombic triacontahedron*	2	7	70,94
	60	$2\ \frac{5}{2}\|3$	$(6.6.\frac{5}{2})$	great truncated icosahedron *great stellapentakisdodecahedron*	2	7	71,95
	61	$2\ \frac{5}{2}\ 3\|$	$(6.4.\frac{6}{5}.\frac{4}{3})$	rhombicosahedron *rhombicosacron*	−10*		72,96
	62	$\|2\ \frac{5}{2}\ 3$	$(3.3.\frac{5}{2}.3.3)$	great snub icosidodecahedron *great pentagonal hexecontahedron*	2	7	73,113
I_9	63	$2\ 5\|\frac{5}{3}$	$(\frac{10}{3}.\frac{10}{3}.5)$	small stellated truncated dodecahedron *great pentakisdodekahedron*	−6	9	74,97
	64	$\frac{5}{3}\ 2\ 5\|$	$(\frac{10}{3}.4.10)$	truncated dodecadodecahedron *medial disdyakistriacontahedron*	−6	3	75,98
	65	$\|\frac{5}{3}\ 2\ 5$	$(3.\frac{5}{3}.3.3.5)$	inverted snub dodecadodecahedron *medial inverted pentagonal hexecontahedron*	−6	9	76,114
I_{10a}	66	$\frac{5}{2}\ 3\|\frac{5}{3}$	$(\frac{10}{3}.\frac{5}{2}.\frac{10}{3}.3)$	great dodecicosidodecahedron *great dodecacronic hexecontahedron*	−16	10	77,99
	67	$\frac{5}{3}\ \frac{5}{2}\|3$	$(6.\frac{5}{3}.6.\frac{5}{2})$	small dodecahemicosahedron *small dodecahemicosacron*	−8*		78,100
	68	$\frac{5}{2}\ \frac{5}{3}\ 3\|$	$(6.\frac{10}{3}.\frac{6}{5}.\frac{10}{7})$	great dodecicosahedron *great dodecicosacron*	−28*		79,101
	69	$\|\frac{5}{3}\ \frac{5}{2}\ 3$	$(3.\frac{5}{3}.3.\frac{5}{2}.3.3)$	great snub dodecicosidodecahedron *great hexagonal hexecontahedron*	−16	10	80,115

Table 7: Icosahedral Uniform Polyhedra							
	fig	symbol		name *dual*	χ	D	ref
I_{10b}	70	$\frac{5}{4}\ 5\vert 3$	$(6.\frac{5}{4}.6.5)$	great dodecahemicosahedron *great dodecahemicosacron*	−8*		81,102
I_{13}	71	$2\ 3\vert\frac{5}{3}$	$(\frac{10}{3}.\frac{10}{3}.3)$	great stellated truncated dodecahedron *great triakisicosahedron*	2	13	83,104
	72	$\frac{5}{3}\ 3\vert 2$	$(4.\frac{5}{3}.4.3)$	great rhombicosidodecahedron *great deltoidal hexecontahedron*	2	13	84,105
	73	$\frac{5}{3}\ 2\ 3\vert$	$(\frac{10}{3}.4.6)$	great truncated icosidodecahedron *great disdyakistriacontahedron*	2	13	87,108
	74	$\vert\frac{5}{3}\ 2\ 3$	$(3.\frac{5}{3}.3.3.3)$	great inverted snub icosidodecahedron *great inverted pentagonal hexecontahedron*	2	13	88,116
I_{18a}	75	$\frac{5}{3}\ \frac{5}{2}\vert\frac{5}{3}$	$(\frac{10}{3}.\frac{5}{3}.\frac{10}{3}.\frac{5}{2})$	great dodecahemidodecahedron *great dodecahemidodecacron*	−12*		86,107
I_{18b}	76	$\frac{3}{2}\ 3\vert\frac{5}{3}$	$(\frac{10}{3}.\frac{3}{2}.\frac{10}{3}.3)$	great icosihemidodecahedron *great icosihemidodecacron*	−4*		85,106
I_{22}	77	$\vert\frac{3}{2}\ \frac{3}{2}\ \frac{5}{2}$	$(3.\frac{3}{2}.3.\frac{3}{2}.3.5)$	small retrosnub icosicosidodecahedron *small hexagrammic hexecontahedron*	−8	38	91,118
I_{23}	78	$\frac{3}{2}\ \frac{5}{3}\ 2\vert$	$(4.\frac{10}{3}.\frac{4}{3}.\frac{10}{7})$	great rhombidodecahedron *great rhombidodecacron*	−18*		89,109
	79	$\vert\frac{3}{2}\ \frac{5}{3}\ 2$	$(3.\frac{3}{2}.3.\frac{5}{3}.3)$	great retrosnub icosidodecahedron *great pentagrammic hexecontahedron*	2	37	90,117

Table 8: Non-Wythoffian Uniform Polyhedra						
fig	symbol		name *dual*	χ	D	ref
80	$\vert\frac{3}{2}\ \frac{5}{3}\ 3\ \frac{5}{2}$	$(4.\frac{5}{3}.4.3.4.\frac{5}{2}.4.\frac{3}{2})$	great dirhombicosidodecahedron *great dirhombicosidodecacron*	−56		92,119

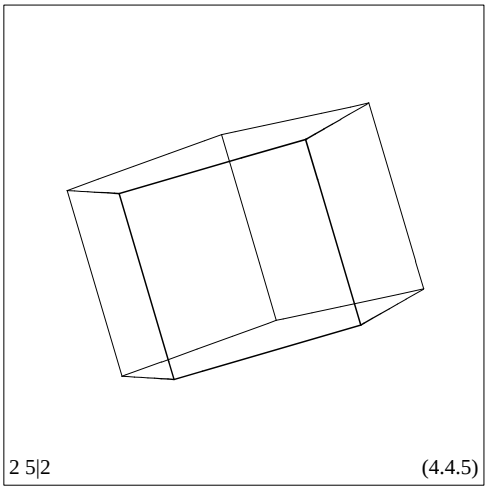

Fig. 1

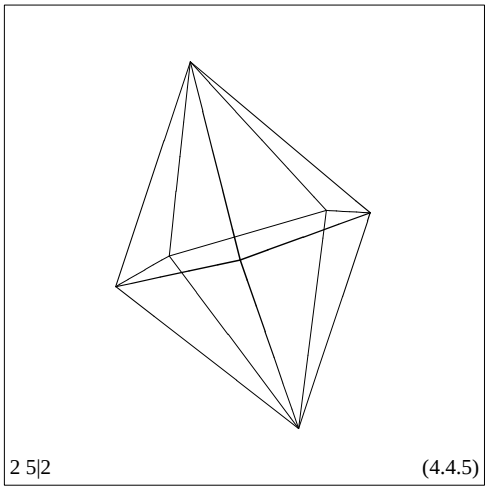

Fig. 1*

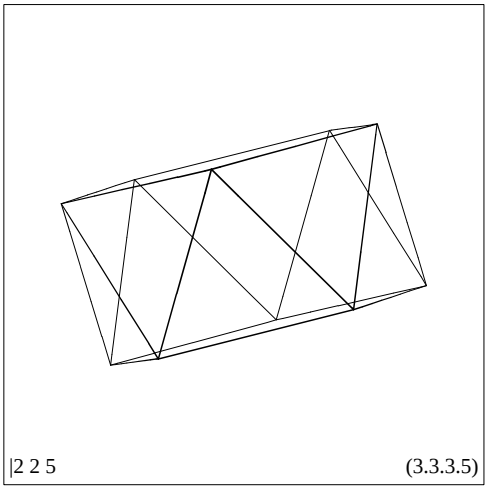

Fig. 2

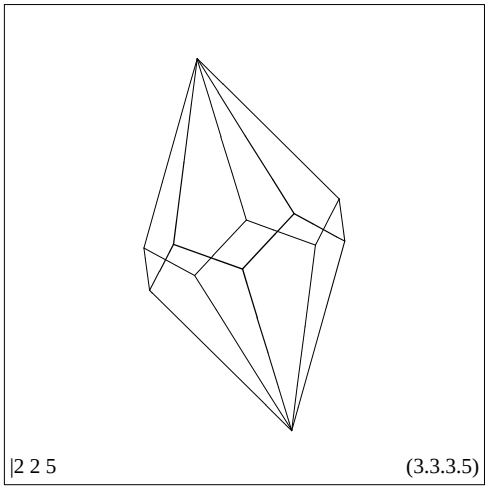

Fig. 2*

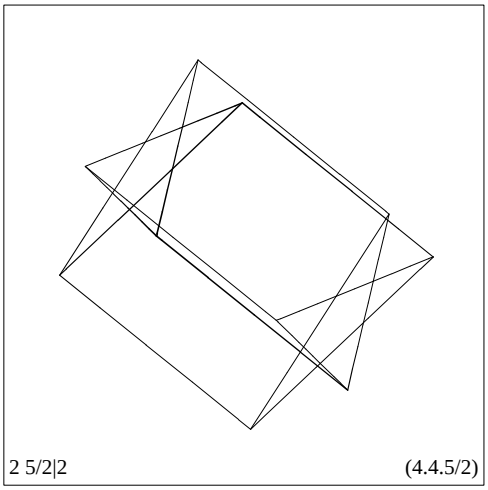

Fig. 3

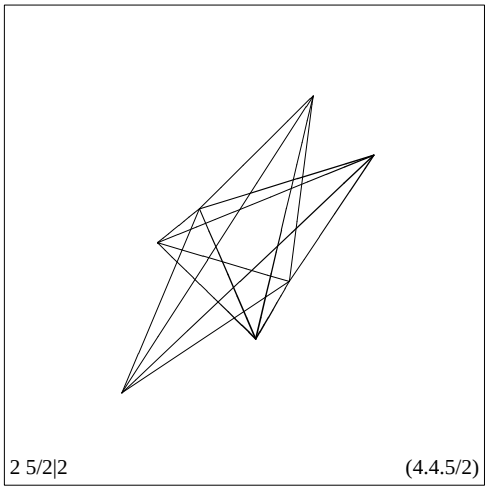

Fig. 3*

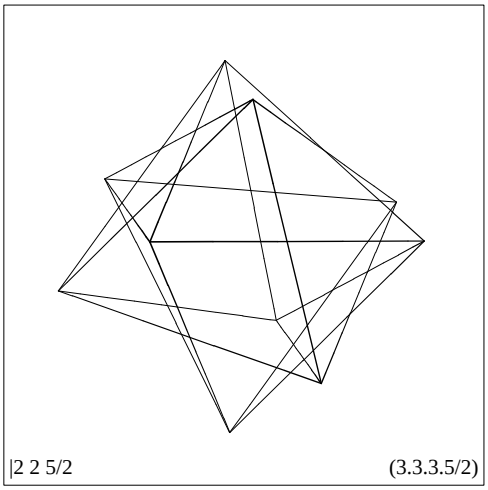

Fig. 4

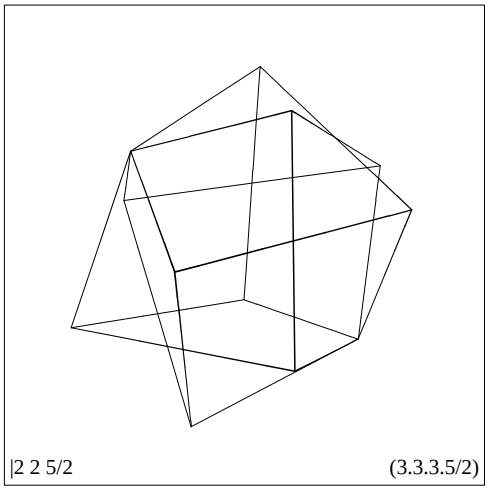

Fig. 4*

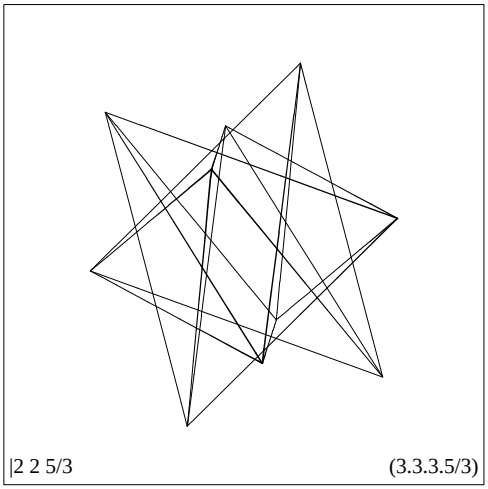

Fig. 5

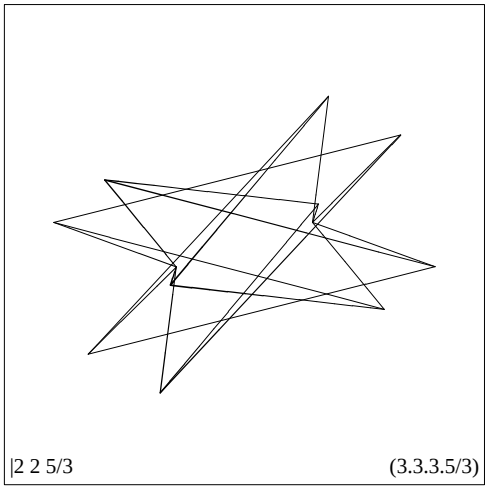

Fig. 5*

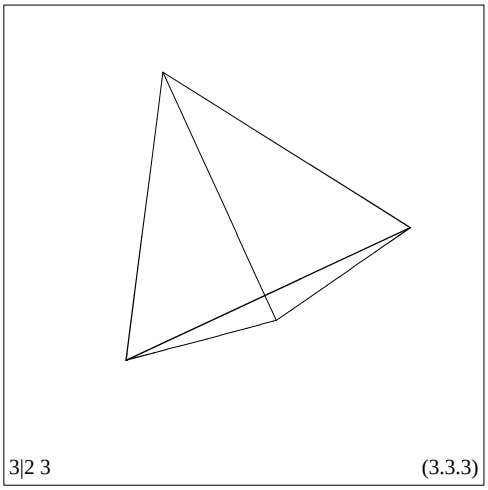

Fig. 6

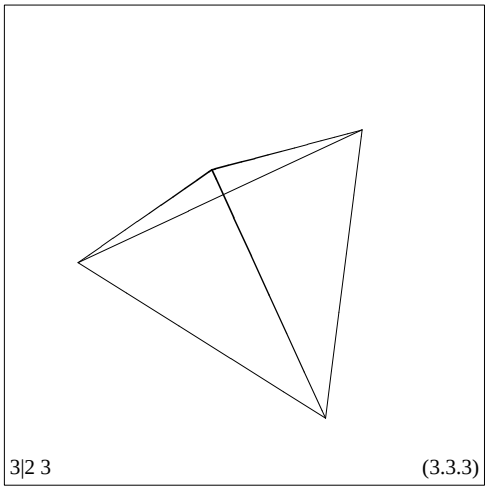

Fig. 6*

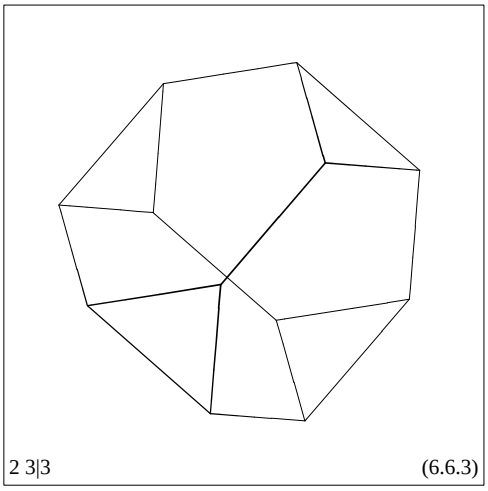

Fig. 7

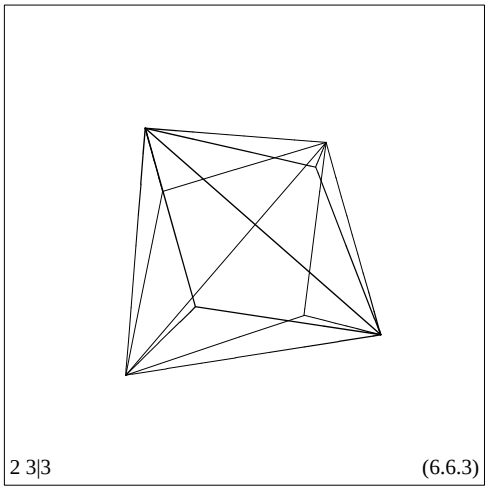

Fig. 7*

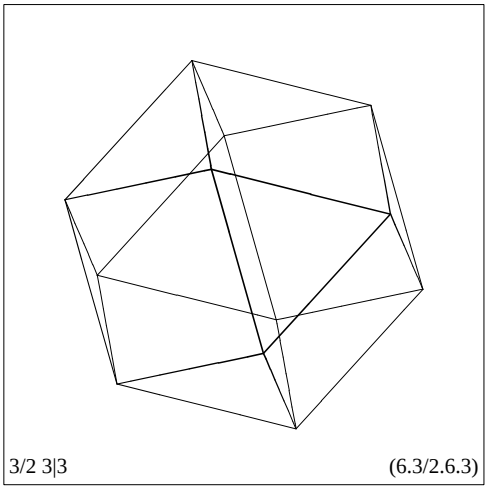

Fig. 8

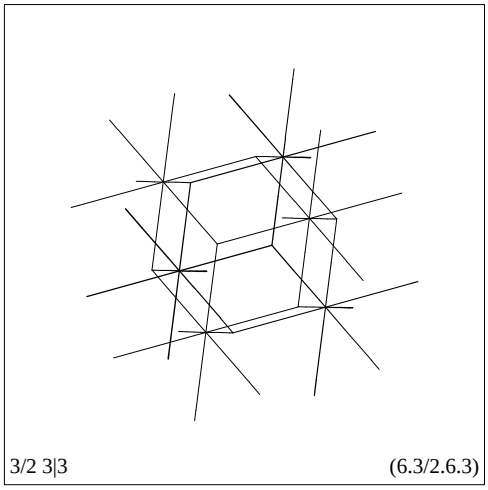

Fig. 8*

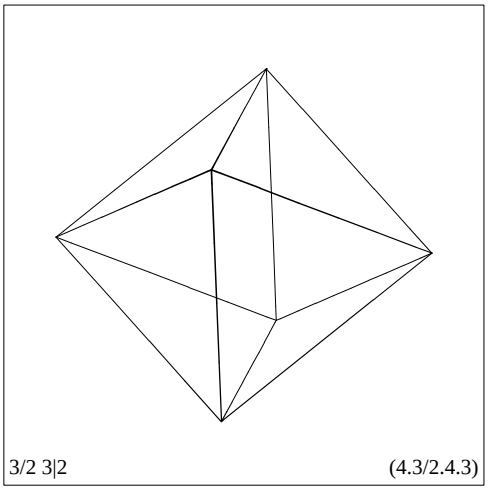

Fig. 9

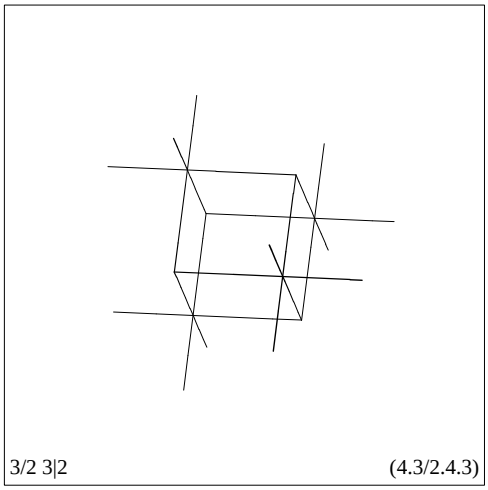

Fig. 9*

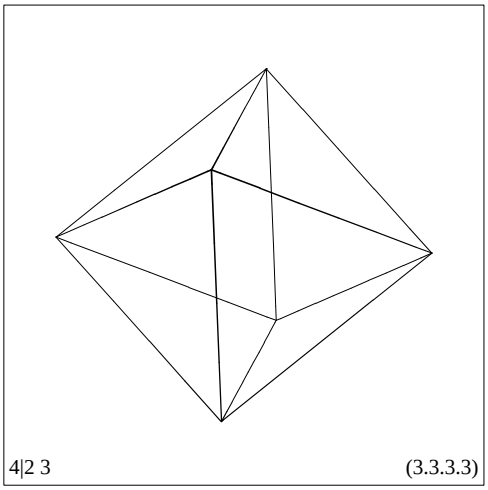

Fig. 10

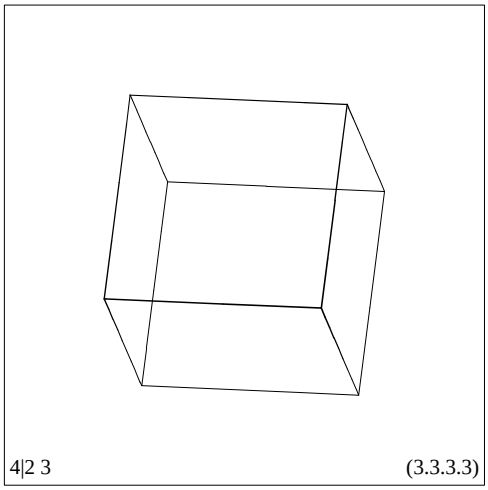

Fig. 10*

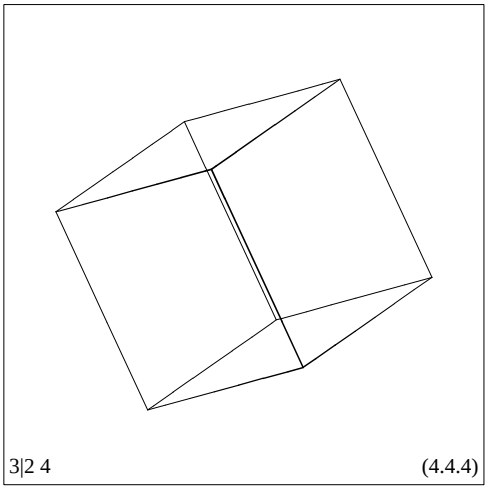

Fig. 11

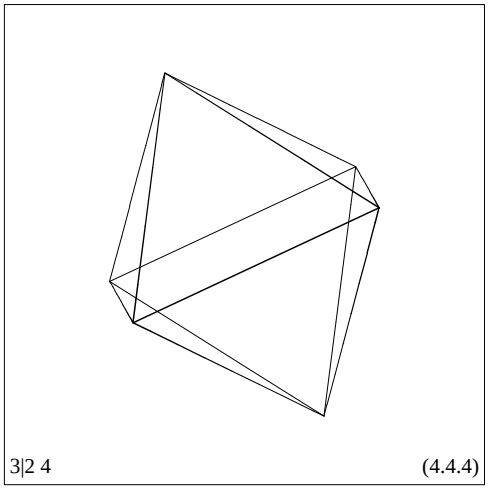

Fig. 11*

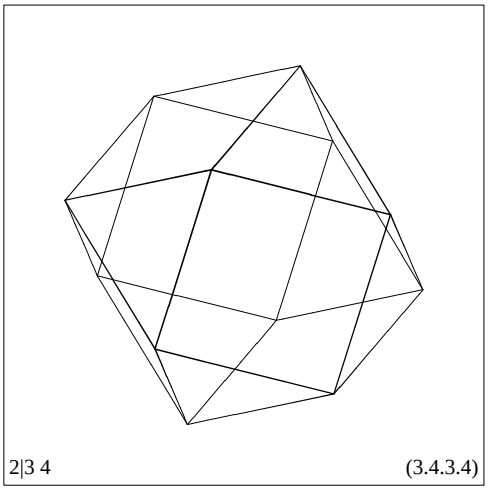

Fig. 12

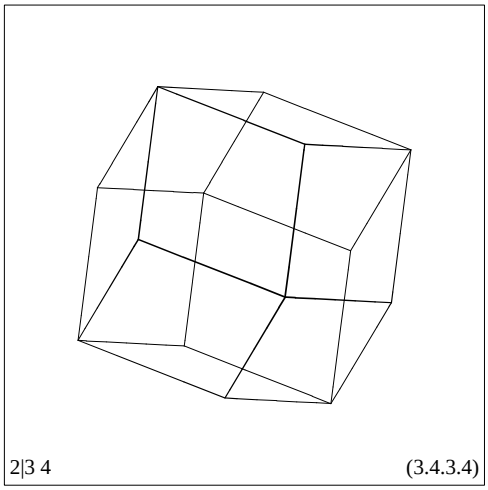

Fig. 12*

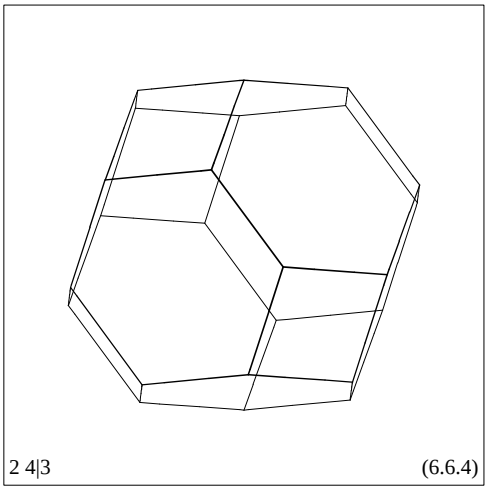

Fig. 13

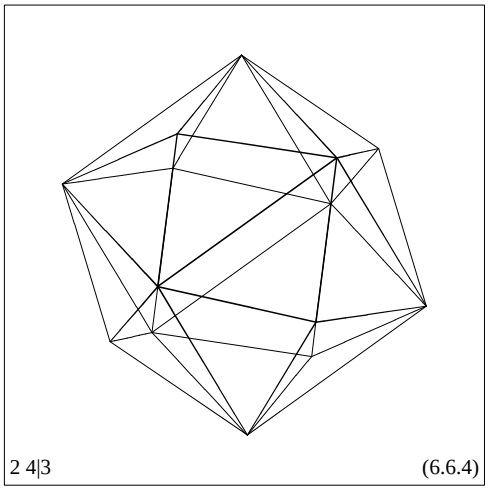

Fig. 13*

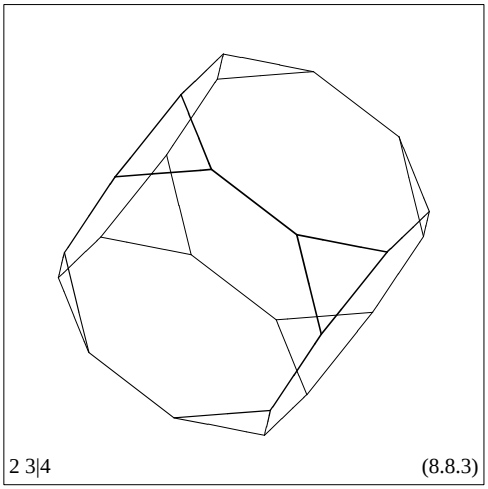

Fig. 14

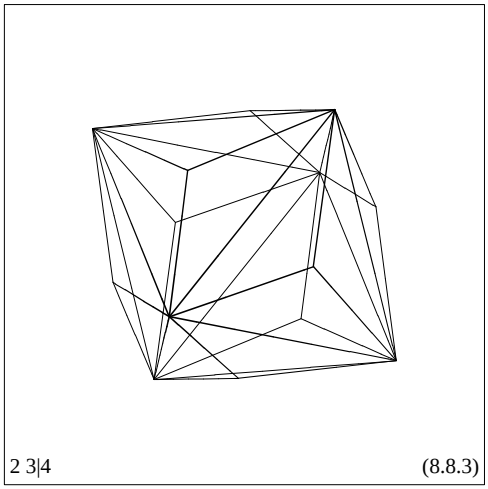

Fig. 14*

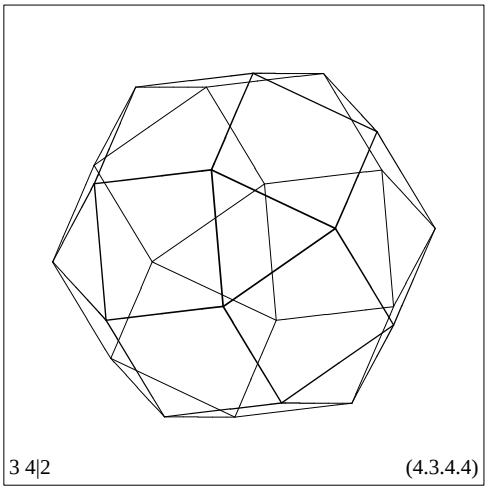

Fig. 15

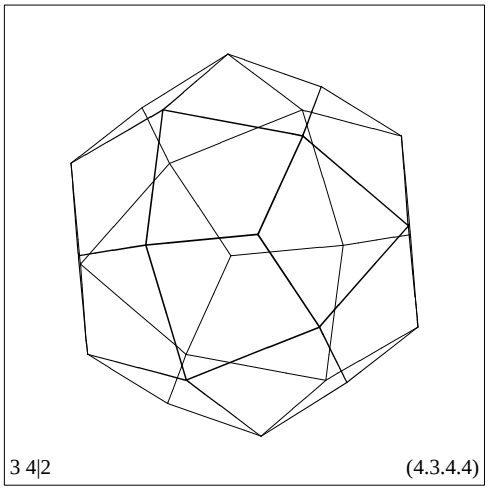

Fig. 15*

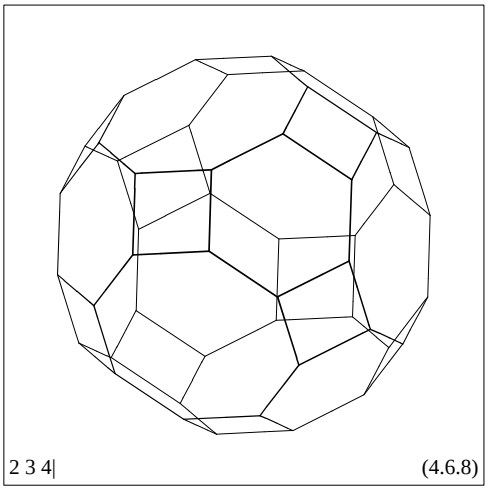

Fig. 16

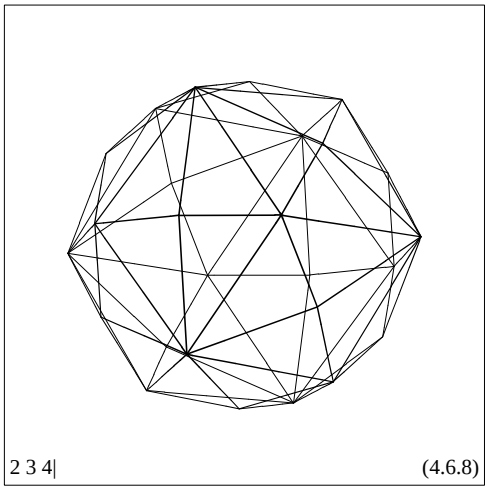

Fig. 16*

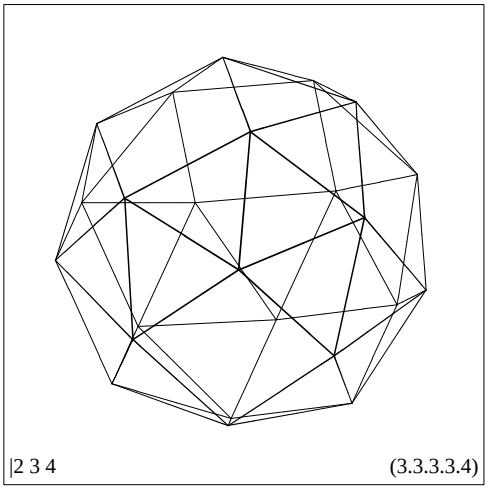

Fig. 17

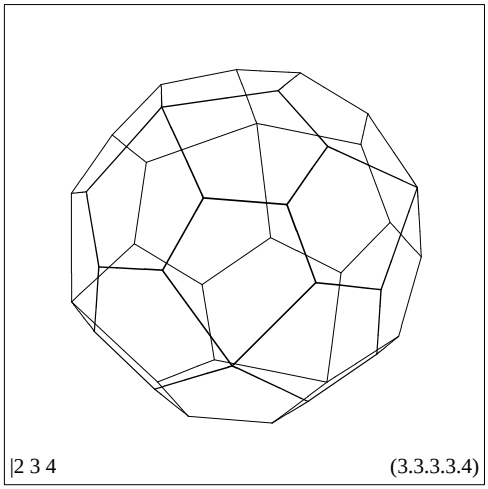

Fig. 17*

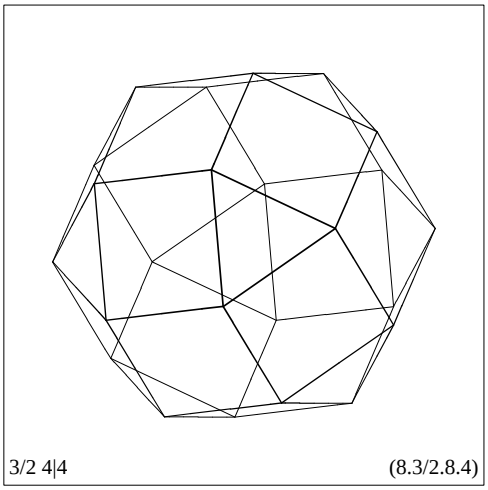

Fig. 18

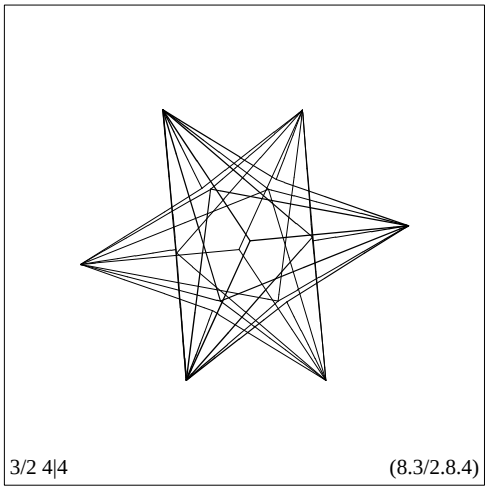

Fig. 18*

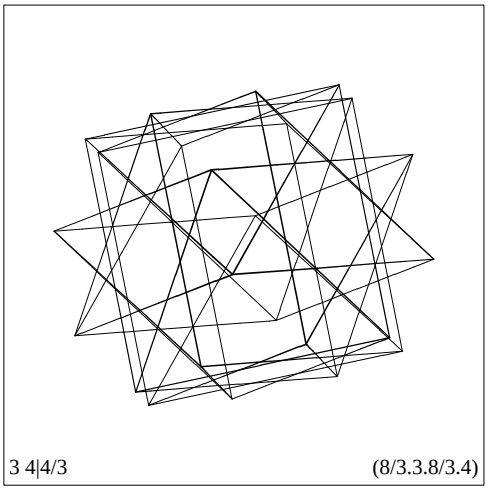

Fig. 19

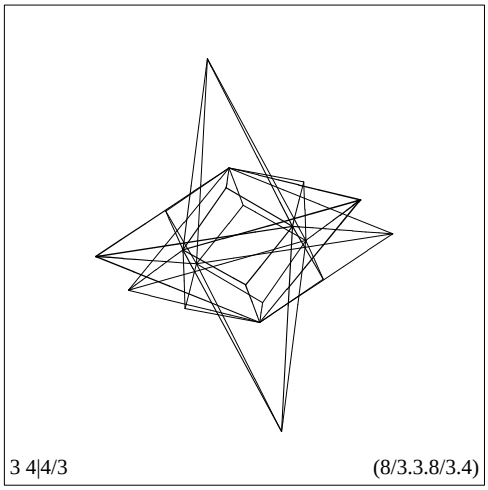

Fig. 19*

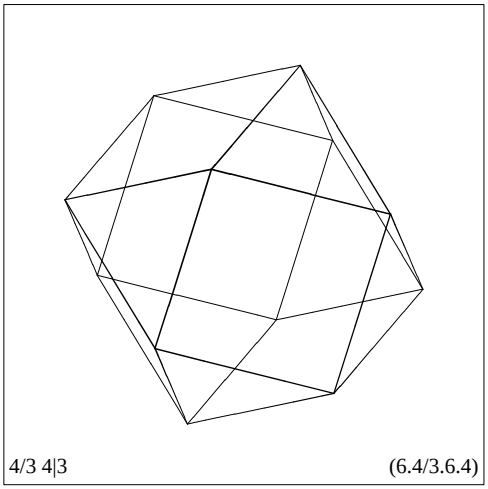

Fig. 20

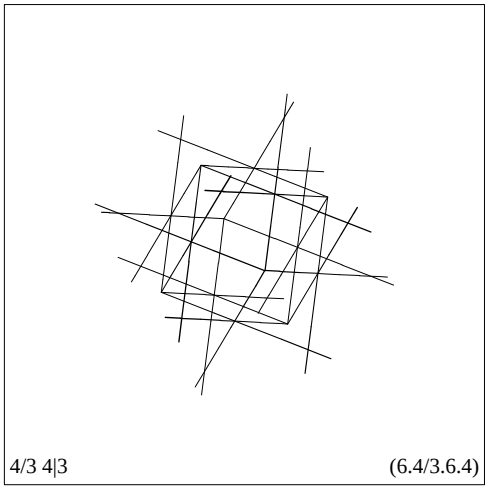

Fig. 20*

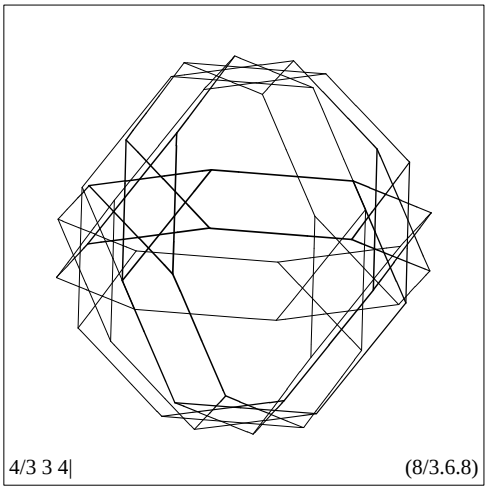

Fig. 21

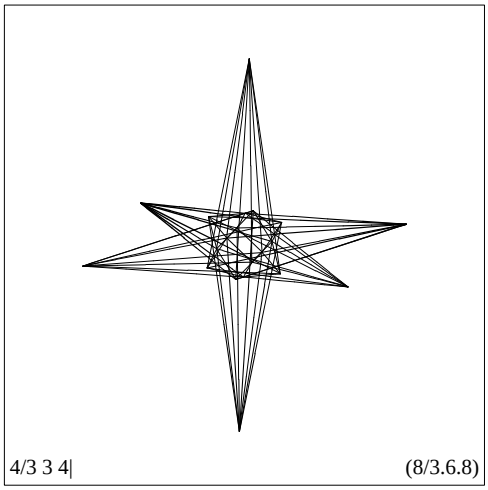

Fig. 21*

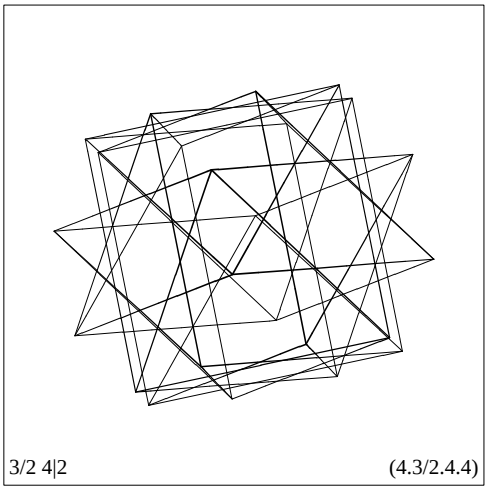

3/2 4|2 (4.3/2.4.4)

Fig. 22

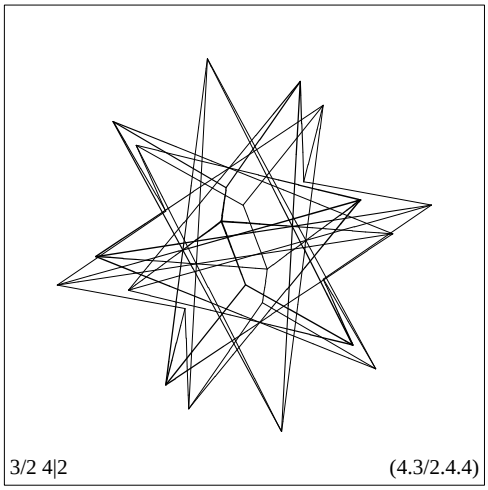

3/2 4|2 (4.3/2.4.4)

Fig. 22*

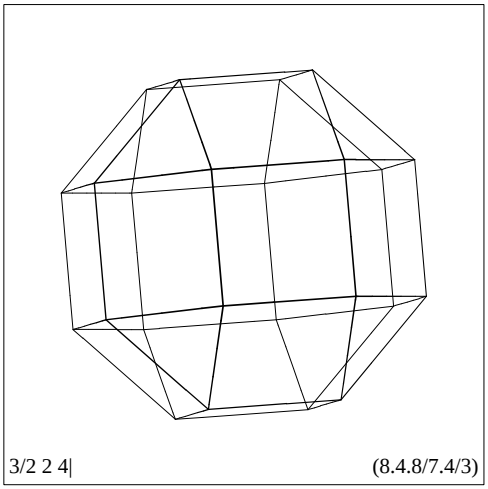

3/2 2 4| (8.4.8/7.4/3)

Fig. 23

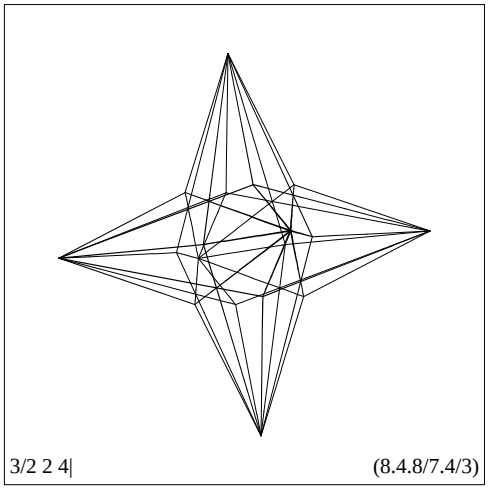

3/2 2 4| (8.4.8/7.4/3)

Fig. 23*

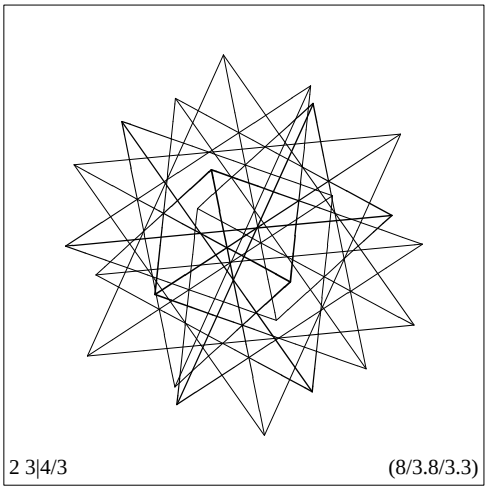

2 3|4/3 (8/3.8/3.3)

Fig. 24

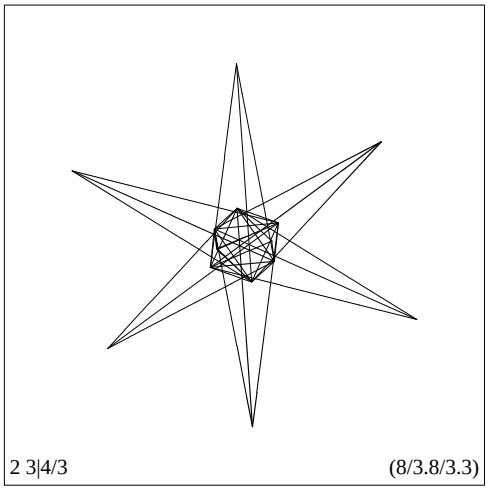

2 3|4/3 (8/3.8/3.3)

Fig. 24*

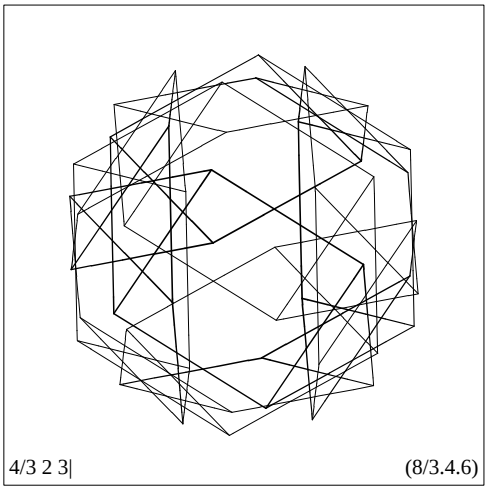

4/3 2 3| (8/3.4.6)

Fig. 25

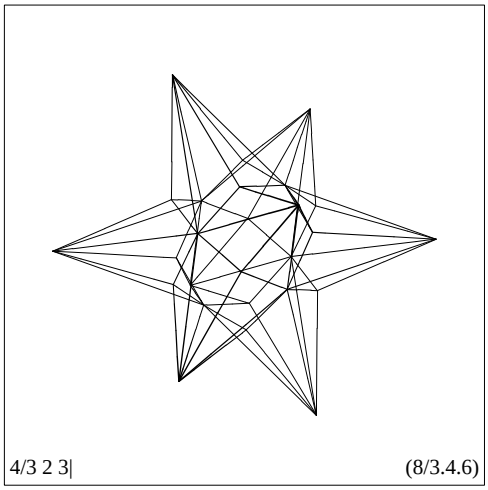

4/3 2 3| (8/3.4.6)

Fig. 25*

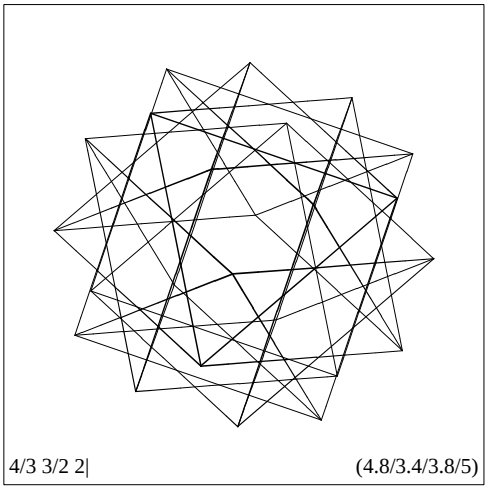

4/3 3/2 2| (4.8/3.4/3.8/5)

Fig. 26

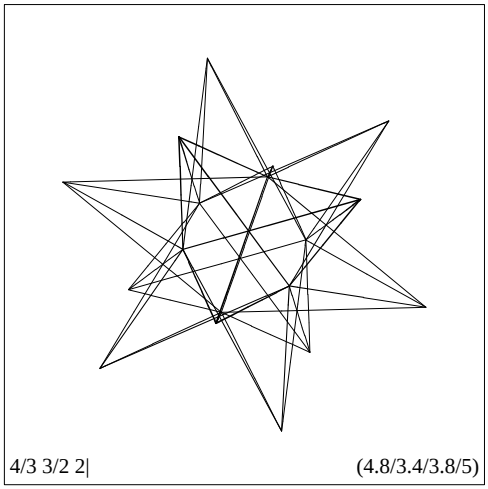

4/3 3/2 2| (4.8/3.4/3.8/5)

Fig. 26*

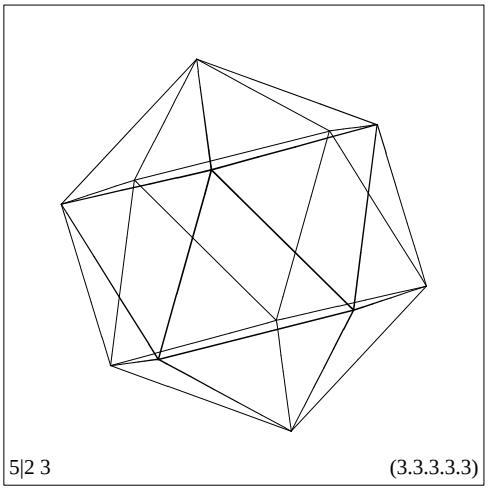

5|2 3 (3.3.3.3.3)

Fig. 27

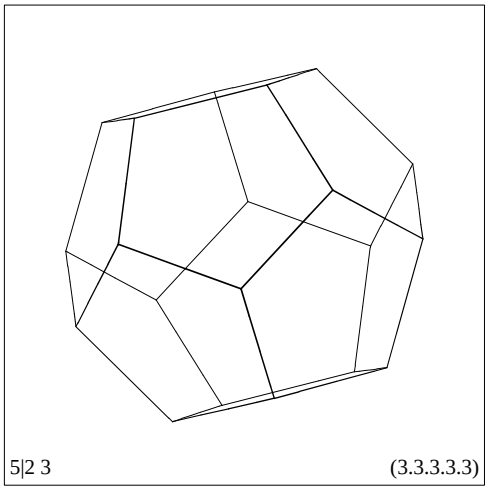

5|2 3 (3.3.3.3.3)

Fig. 27*

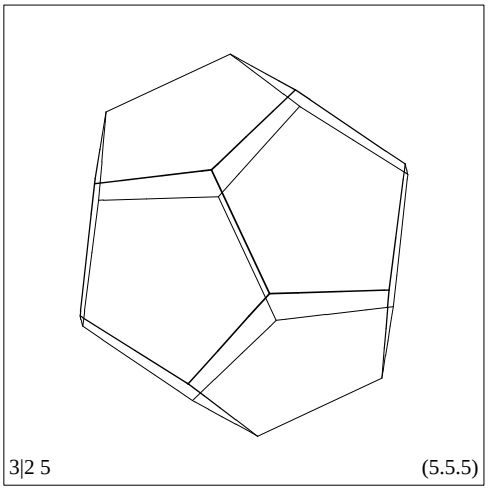

Fig. 28

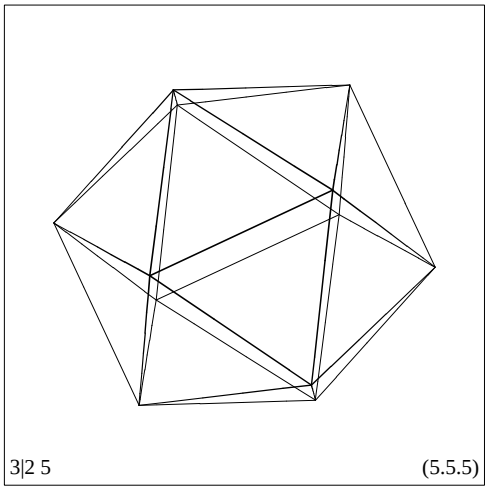

Fig. 28*

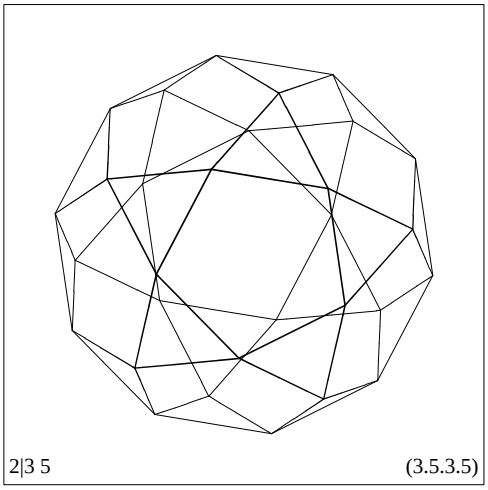

Fig. 29

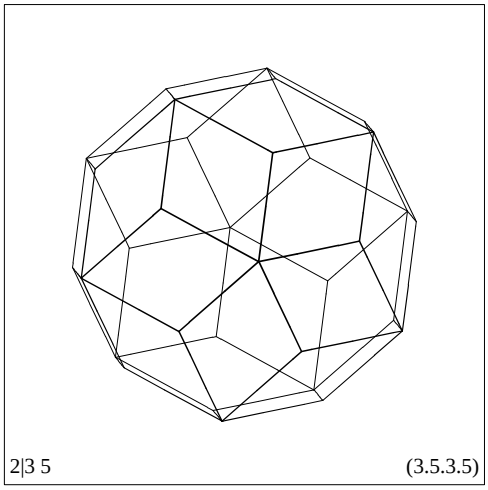

Fig. 29*

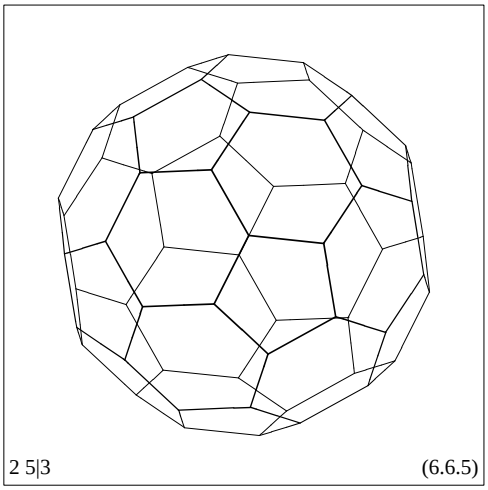

Fig. 30

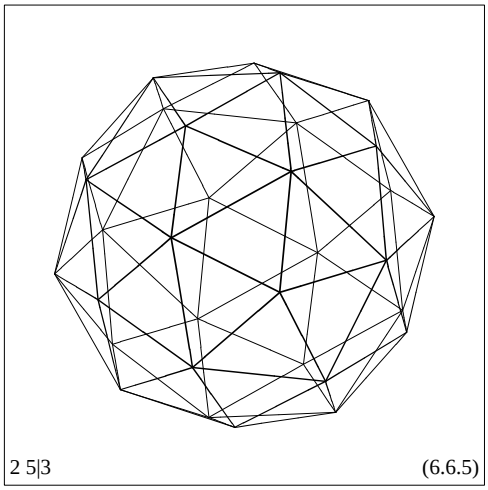

Fig. 30*

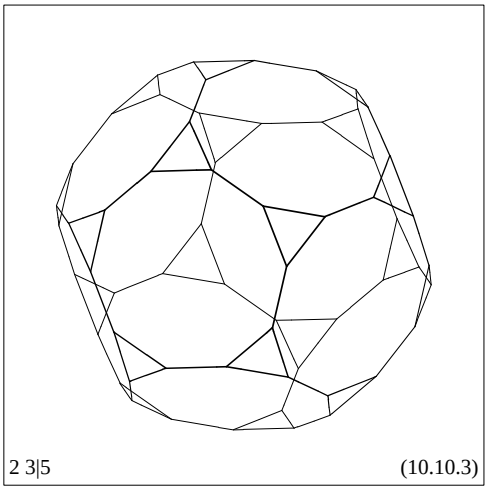

Fig. 31

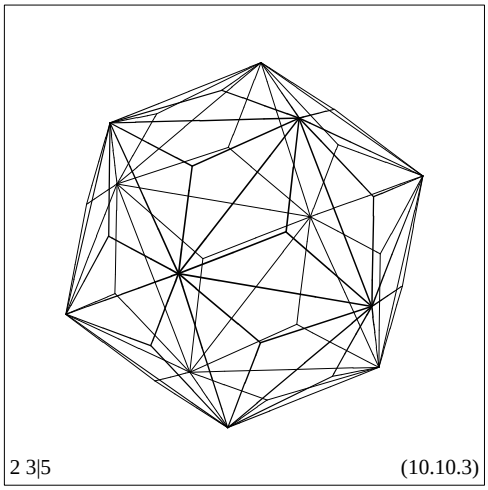

Fig. 31*

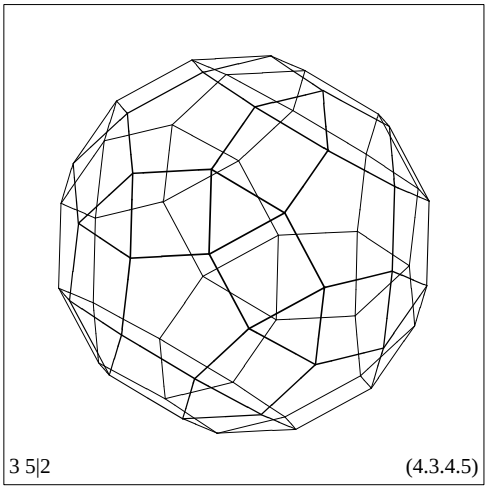

Fig. 32

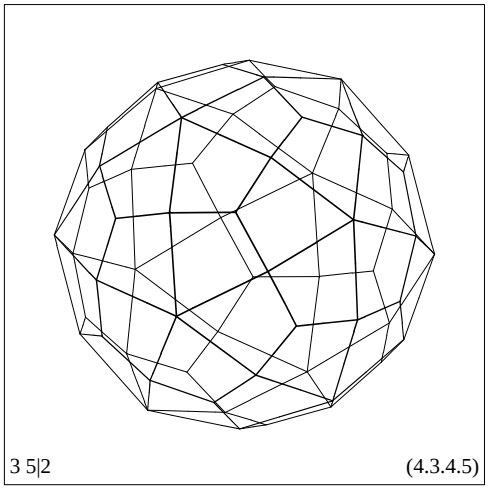

Fig. 32*

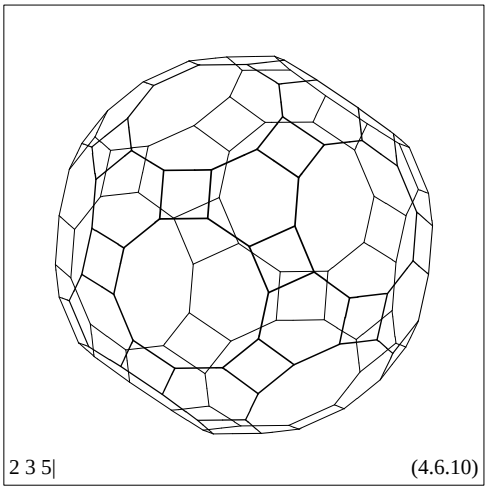

Fig. 33

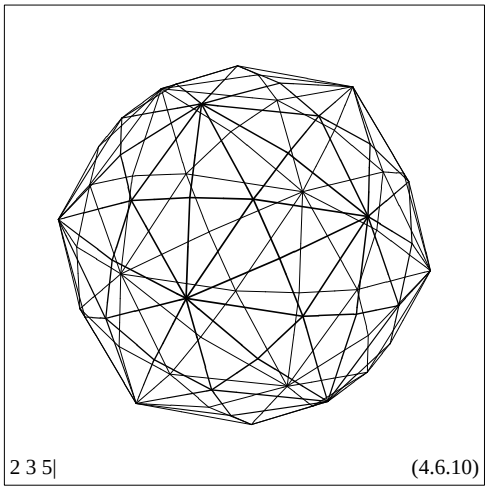

Fig. 33*

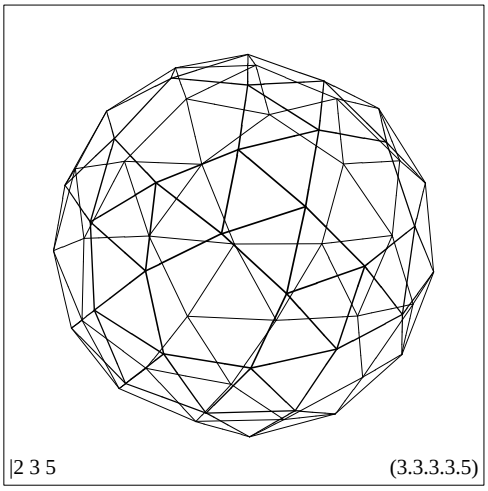

Fig. 34

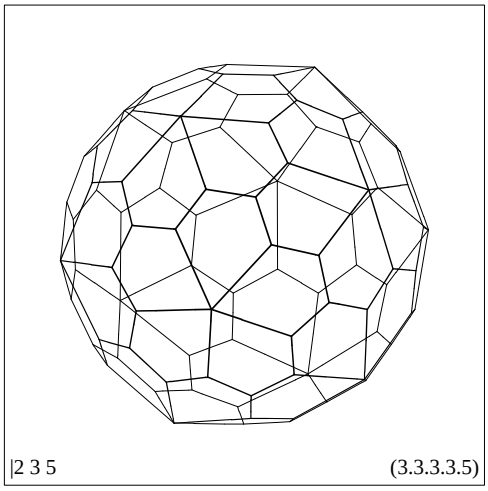

Fig. 34*

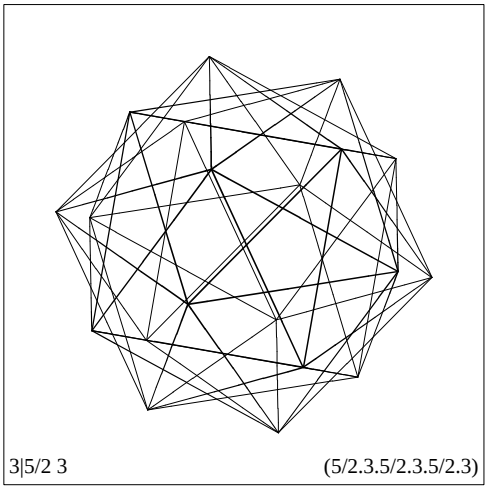

Fig. 35

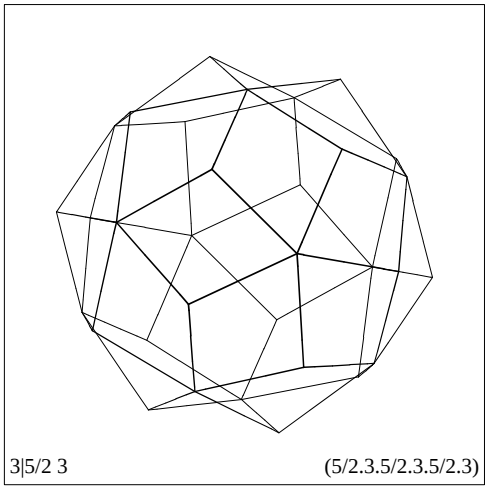

Fig. 35*

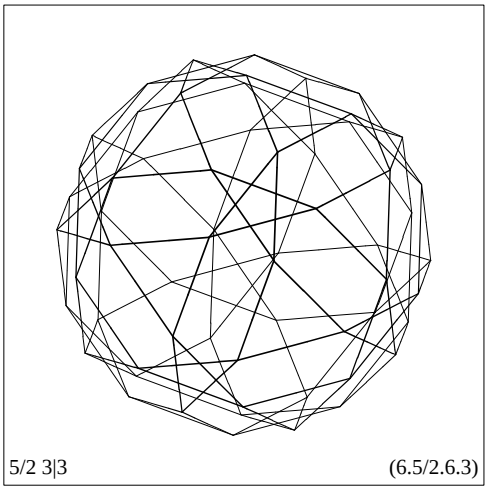

Fig. 36

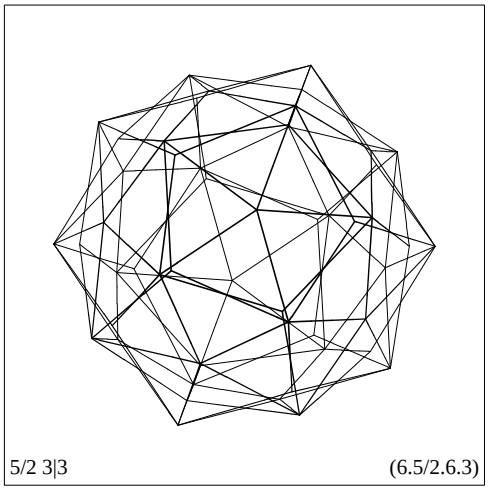

Fig. 36*

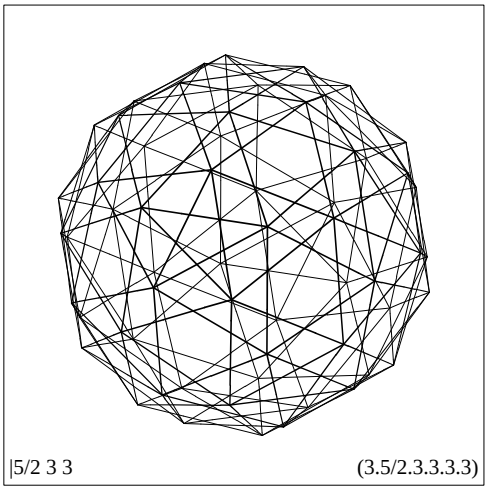

Fig. 37

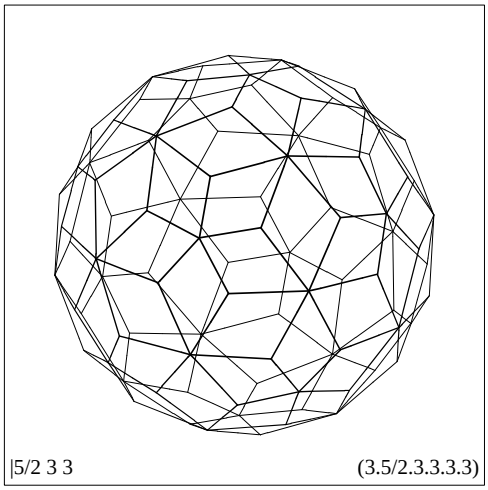

Fig. 37*

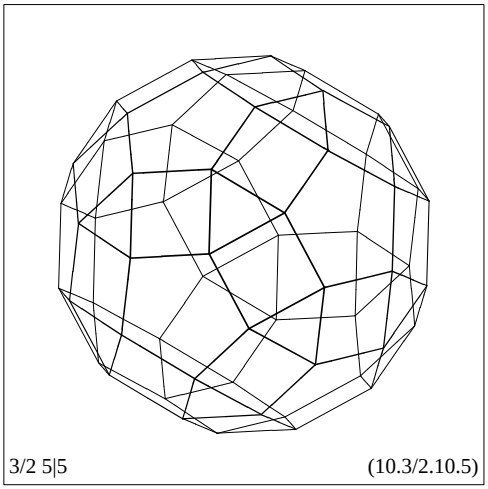

Fig. 38

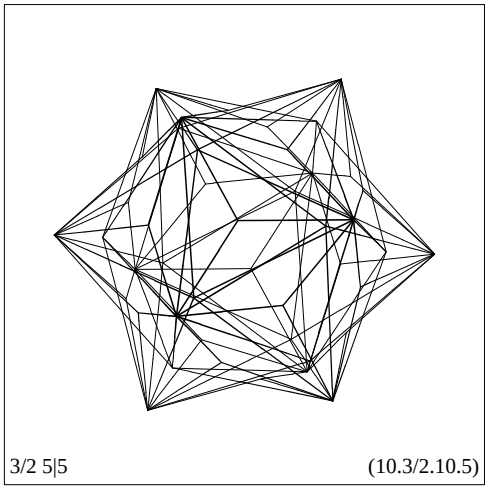

Fig. 38*

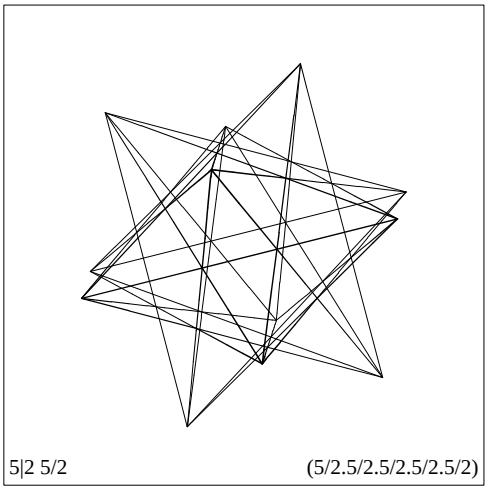

Fig. 39

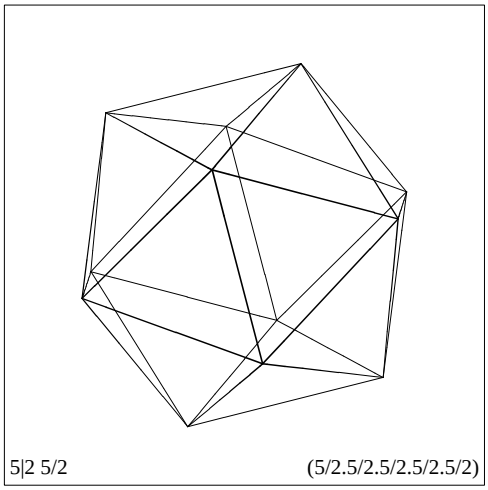

Fig. 39*

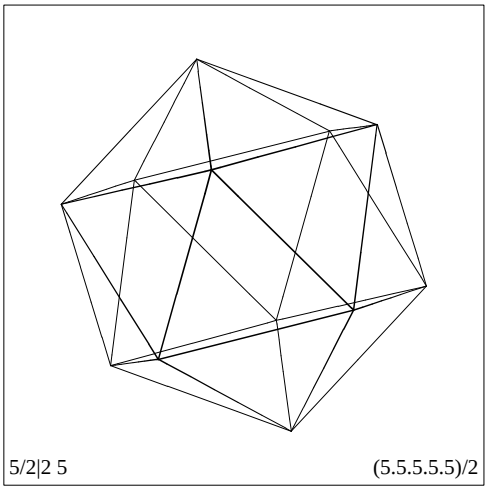

Fig. 40

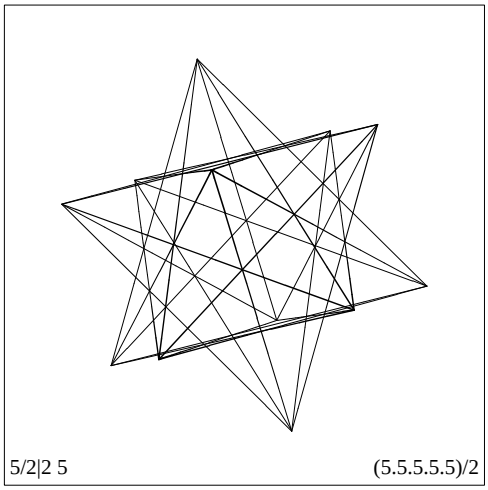

Fig. 40*

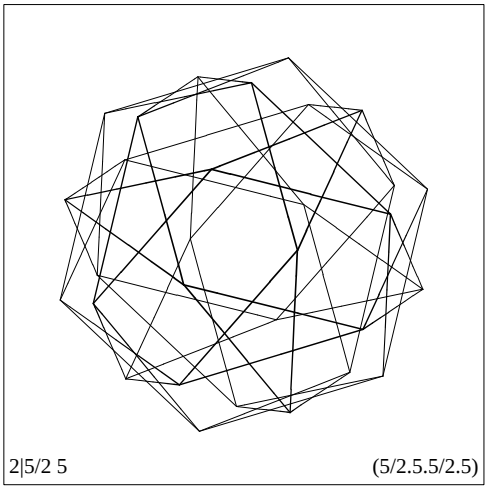

Fig. 41

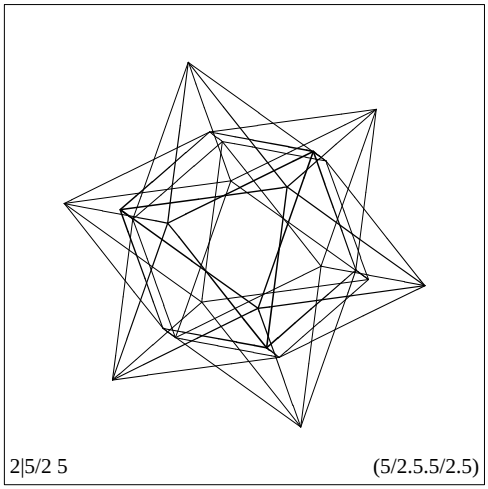

Fig. 41*

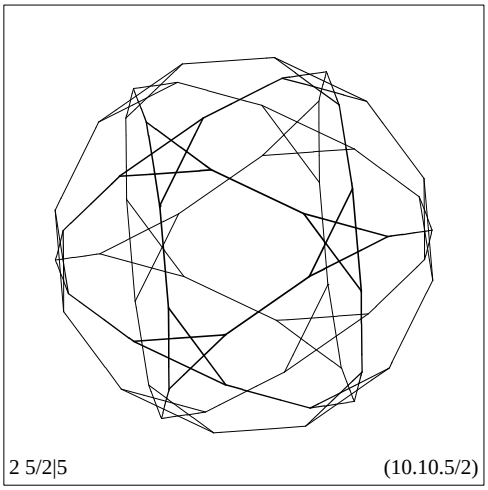

Fig. 42

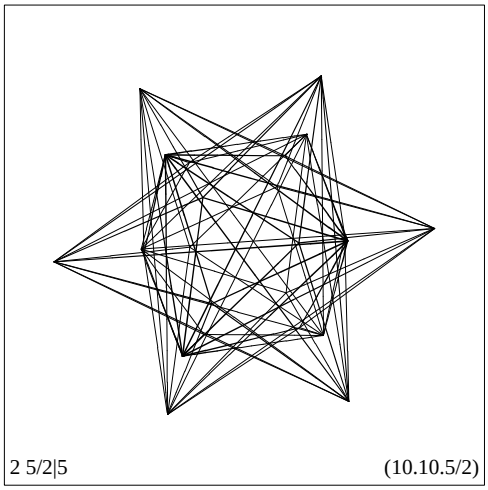

Fig. 42*

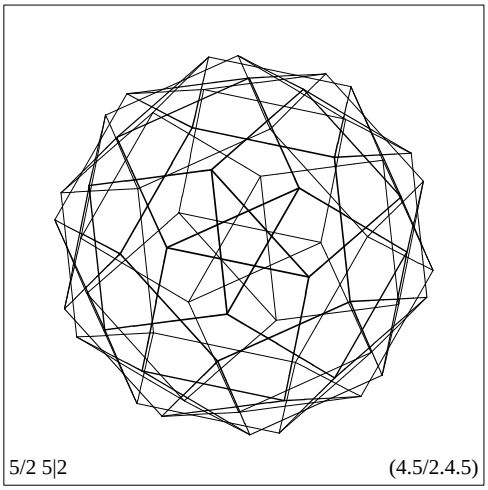

Fig. 43

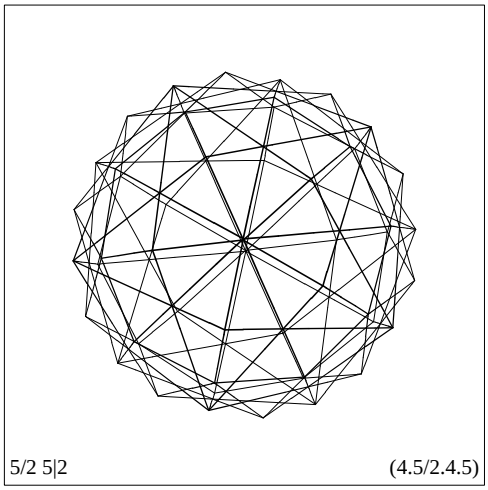

Fig. 43*

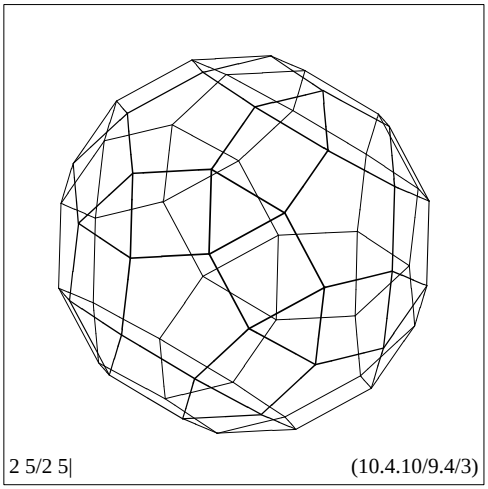

Fig. 44

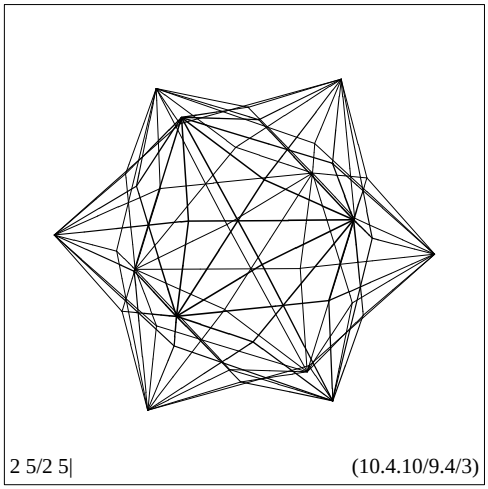

Fig. 44*

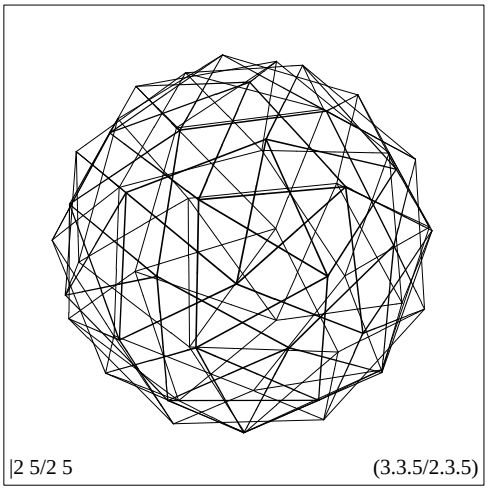

Fig. 45

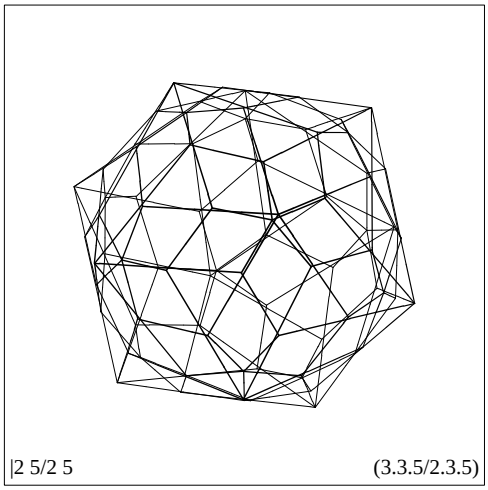

Fig. 45*

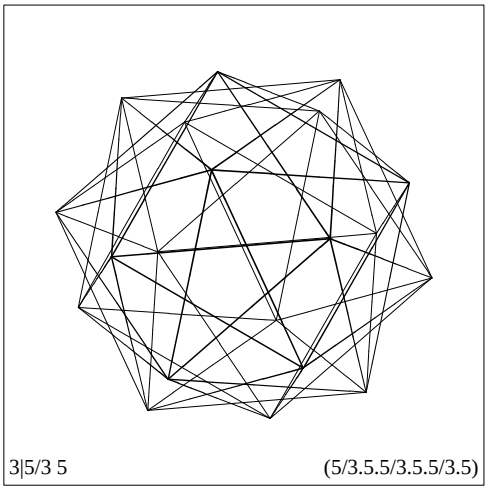

Fig. 46

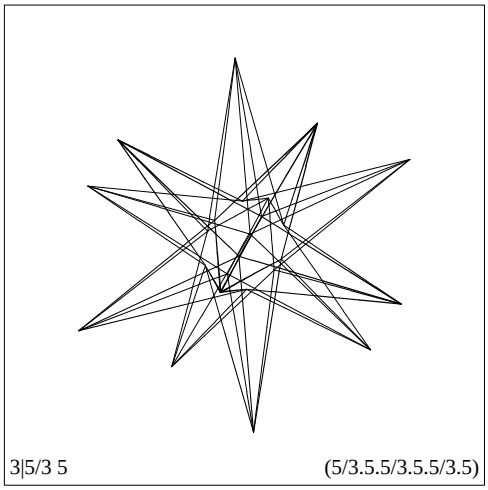

Fig. 46*

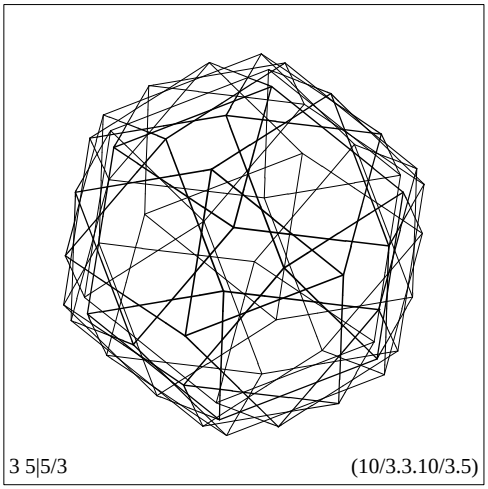

Fig. 47

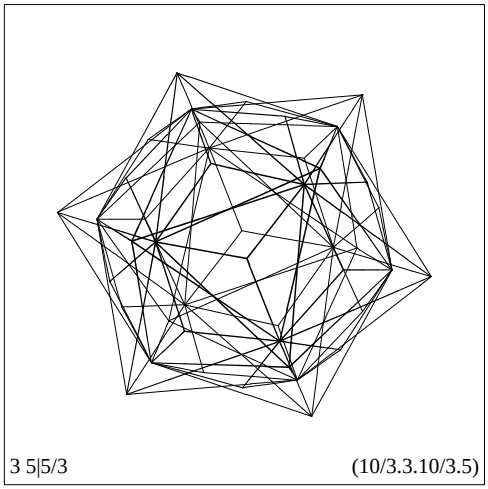

Fig. 47*

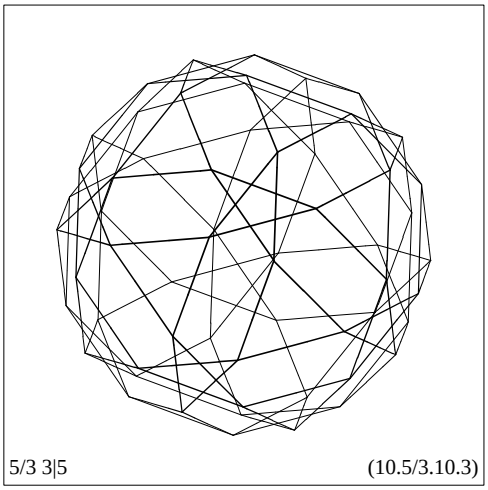

Fig. 48

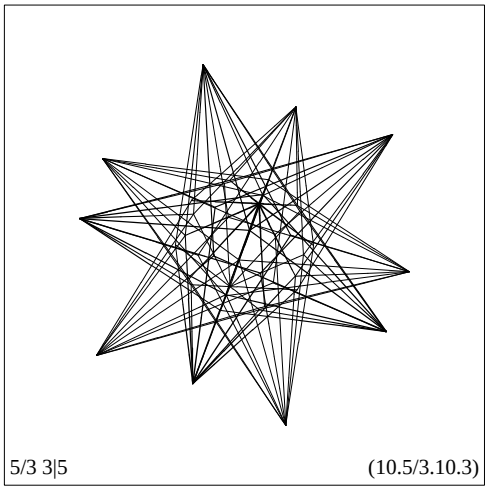

Fig. 48*

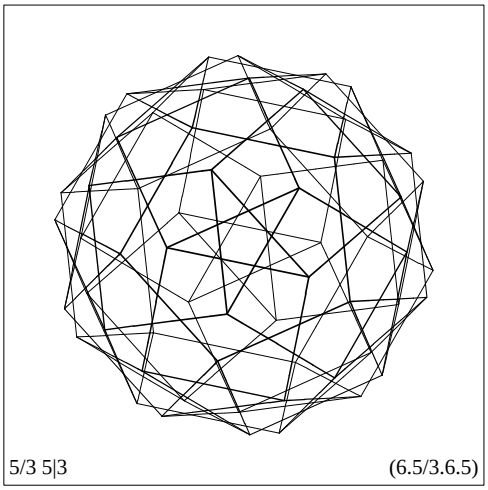

Fig. 49

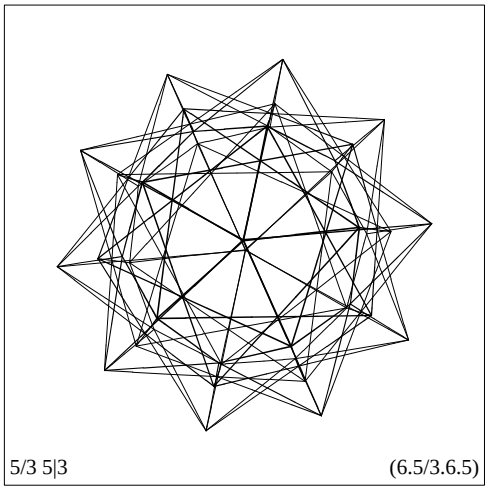

Fig. 49*

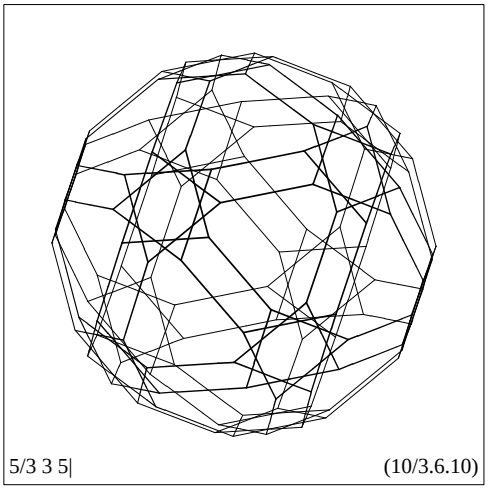

Fig. 50

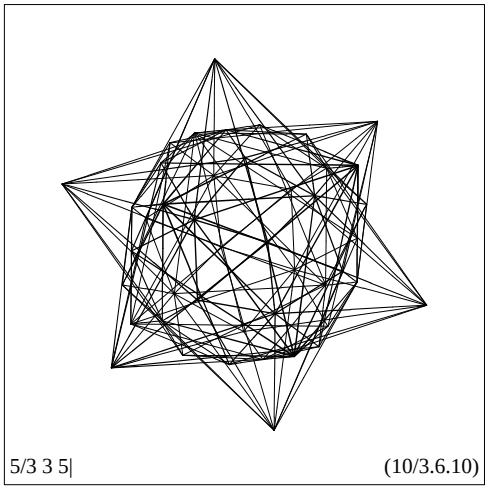

Fig. 50*

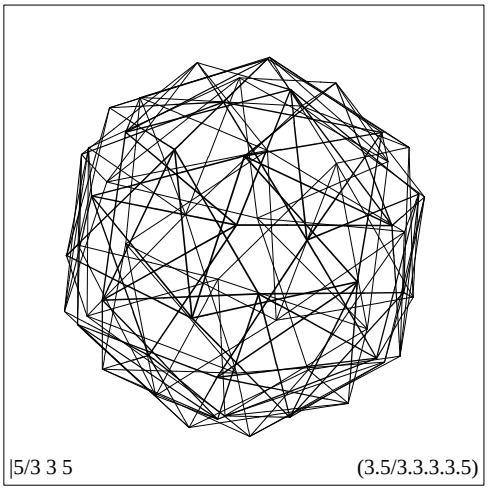

Fig. 51

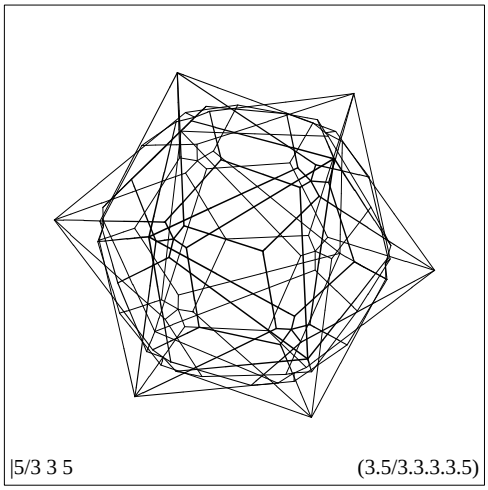

Fig. 51*

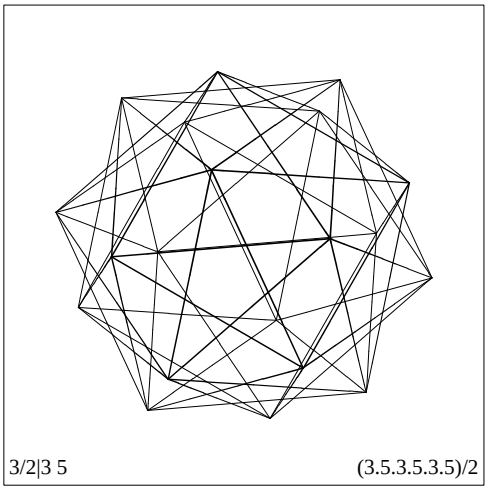

Fig. 52

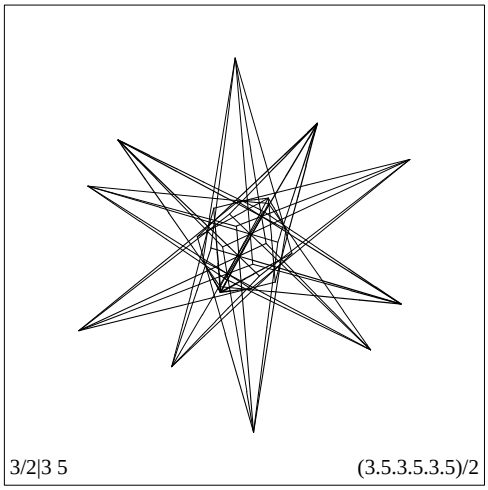

Fig. 52*

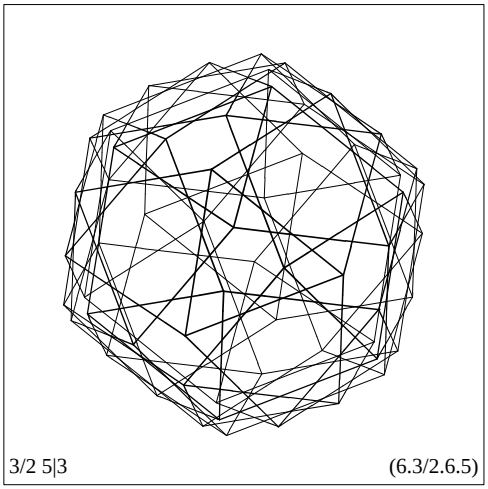

Fig. 53

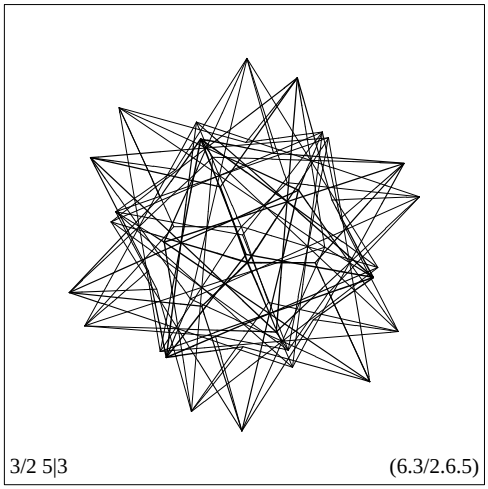

Fig. 53*

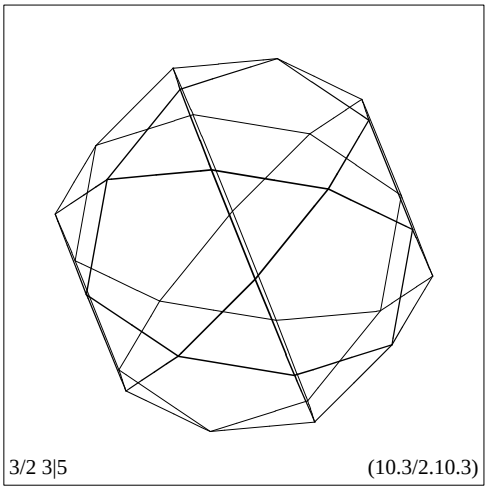

Fig. 54

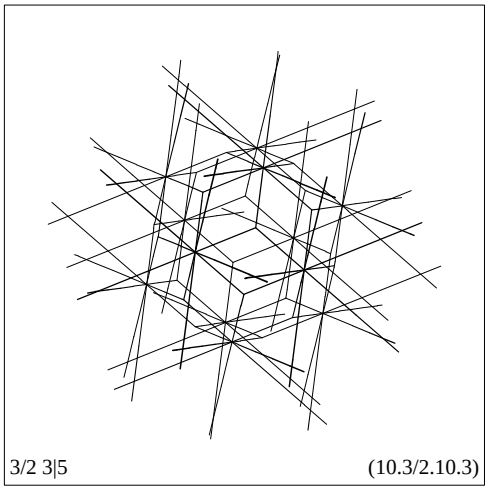

Fig. 54*

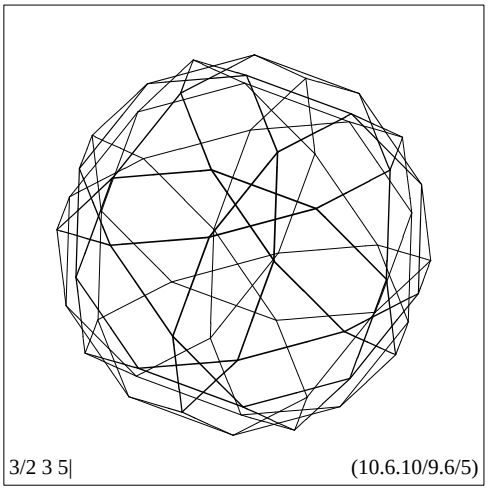

Fig. 55

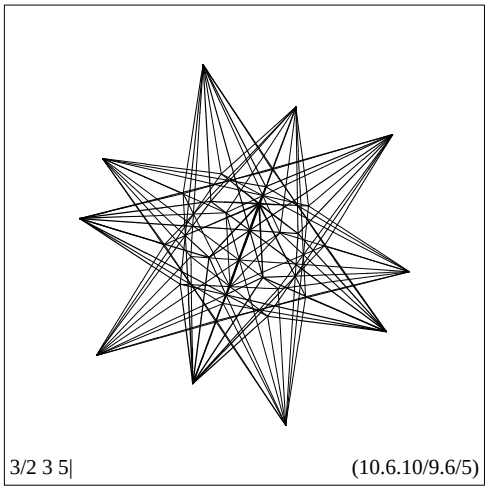

Fig. 55*

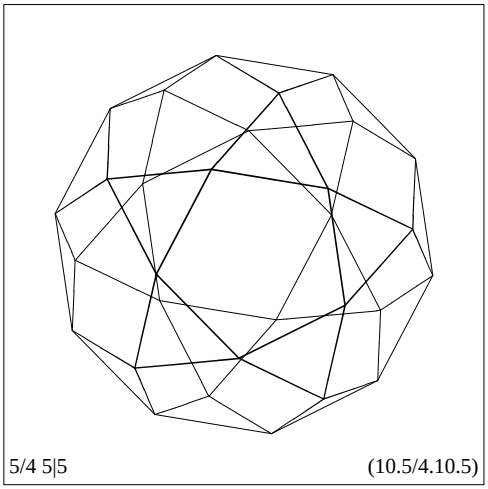

Fig. 56

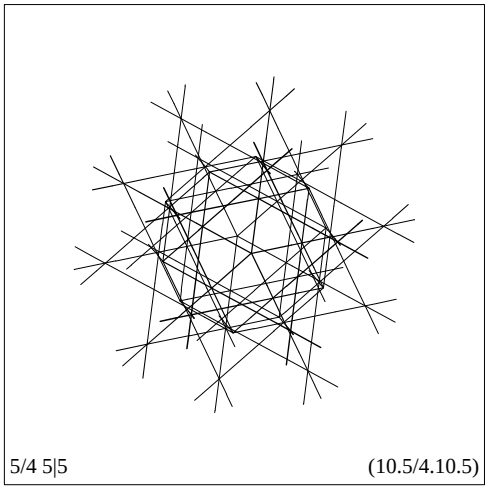

Fig. 56*

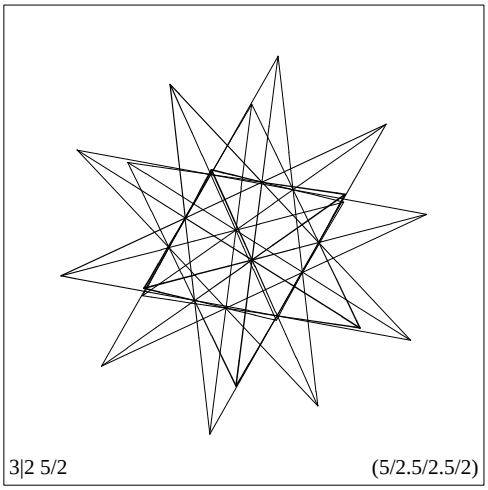

Fig. 57

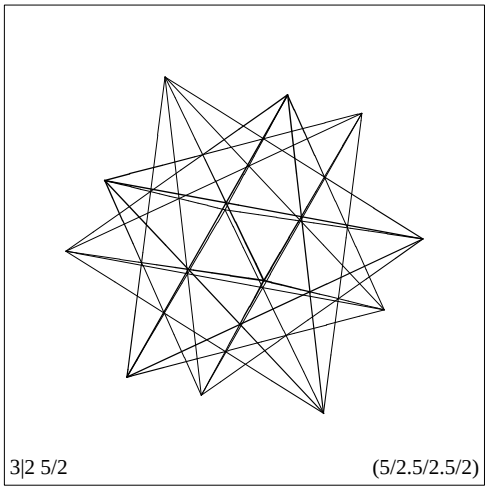

Fig. 57*

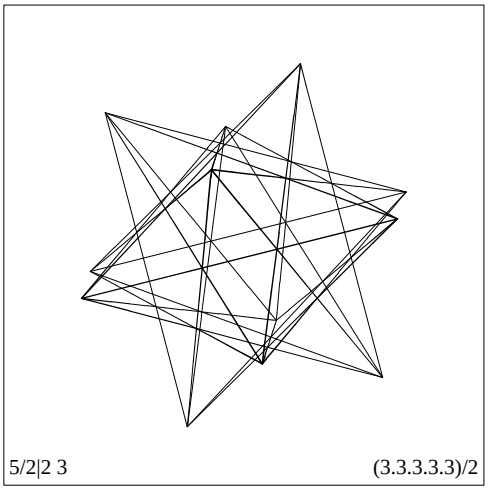

Fig. 58

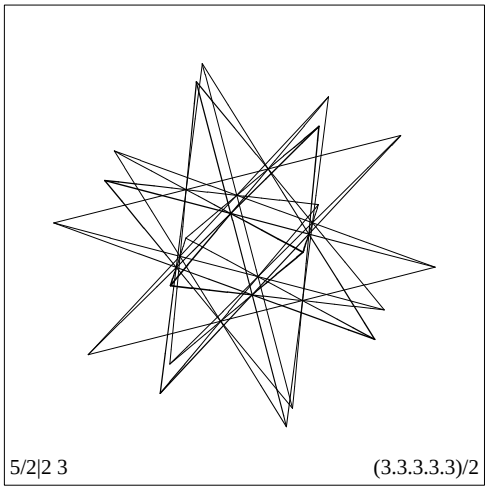

Fig. 58*

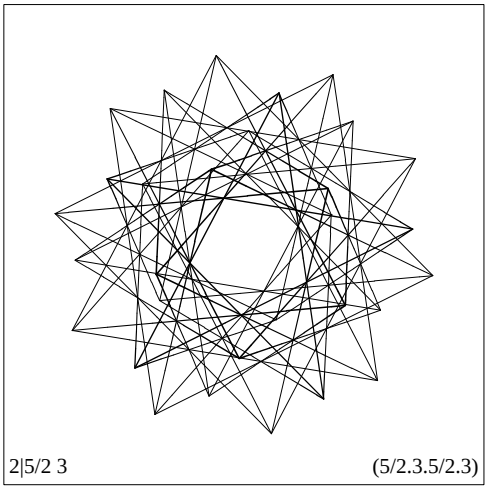

Fig. 59

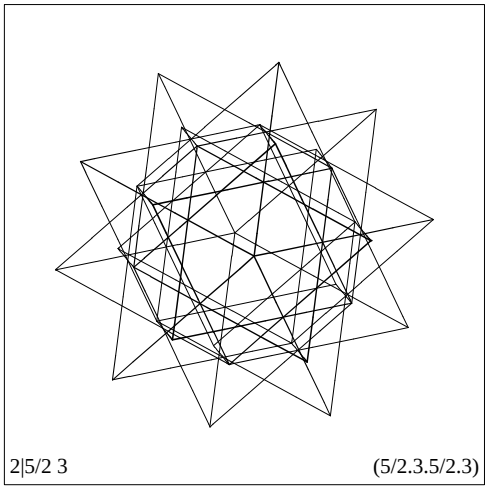

Fig. 59*

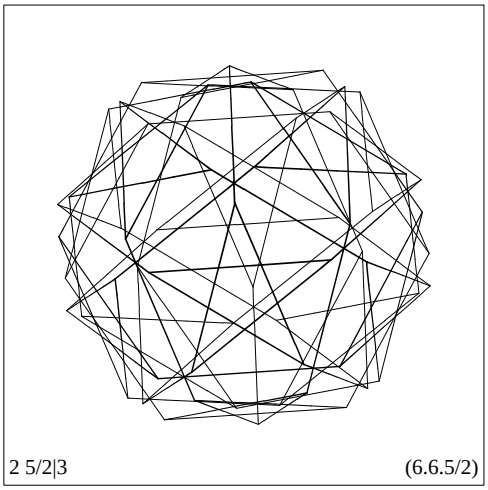

Fig. 60

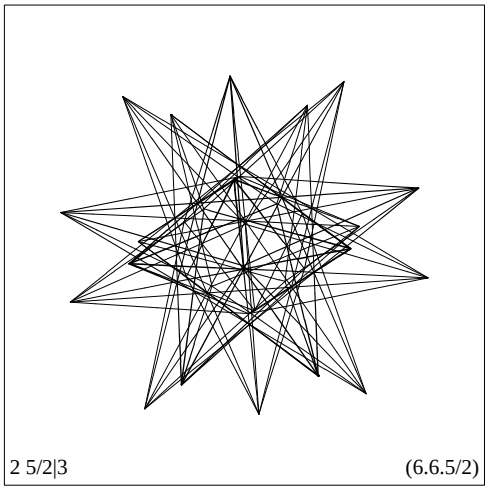

Fig. 60*

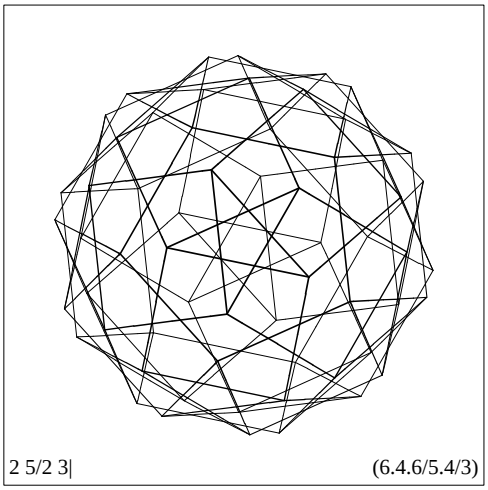

Fig. 61

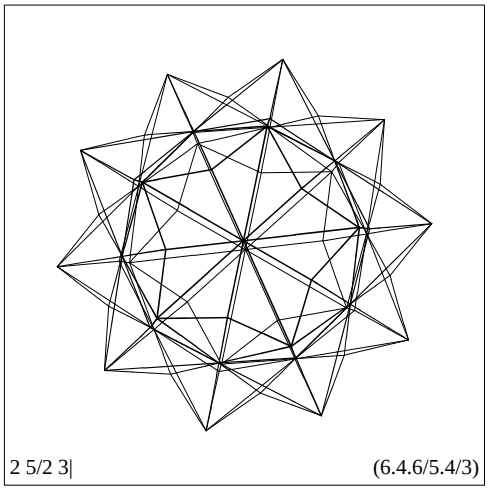

Fig. 61*

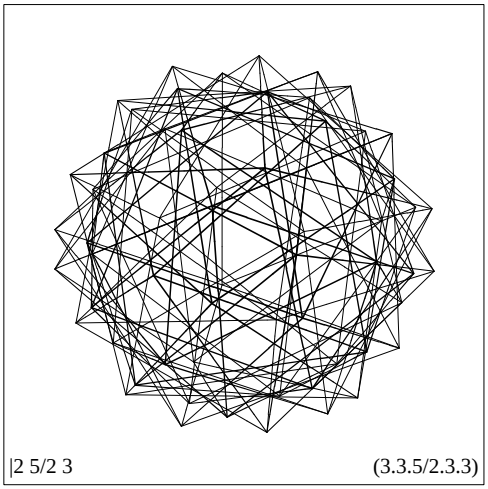

Fig. 62

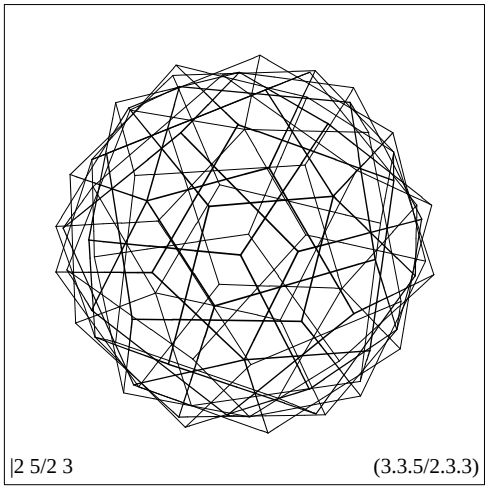

Fig. 62*

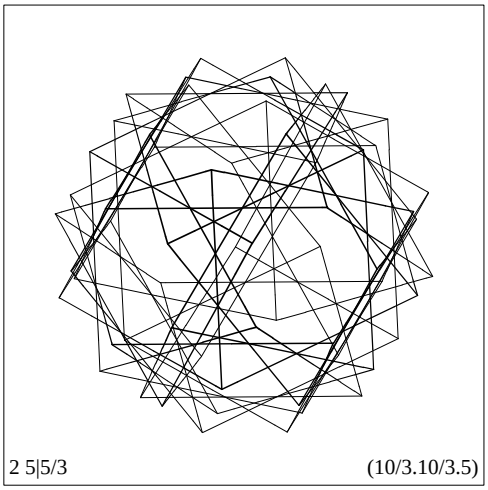

Fig. 63

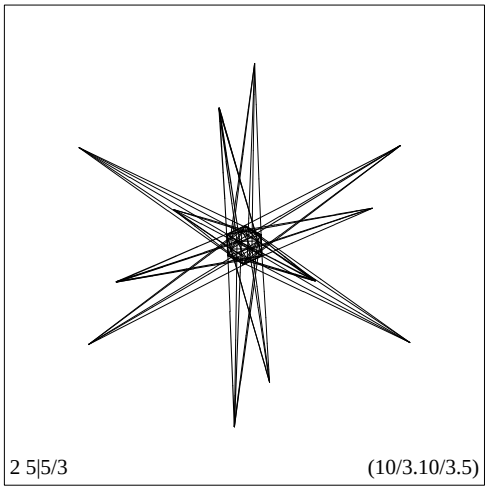

Fig. 63*

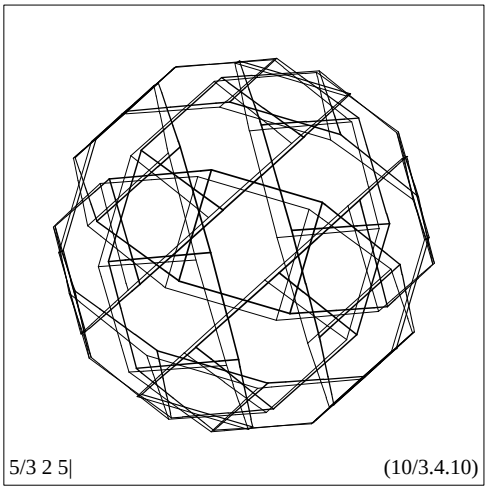

Fig. 64

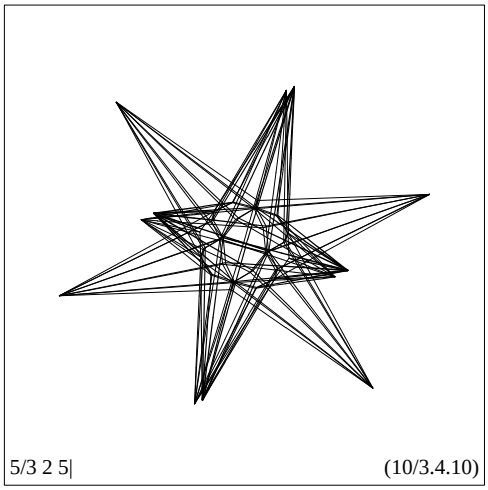

Fig. 64*

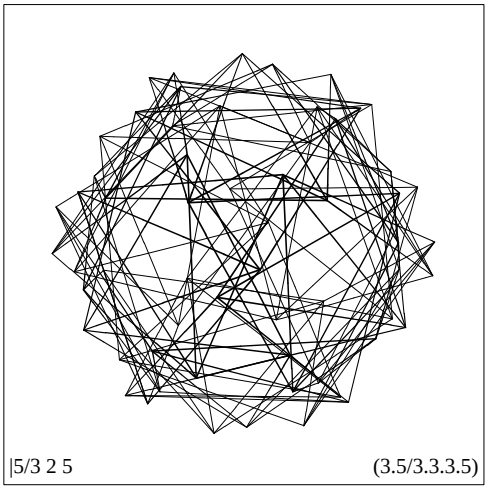

Fig. 65

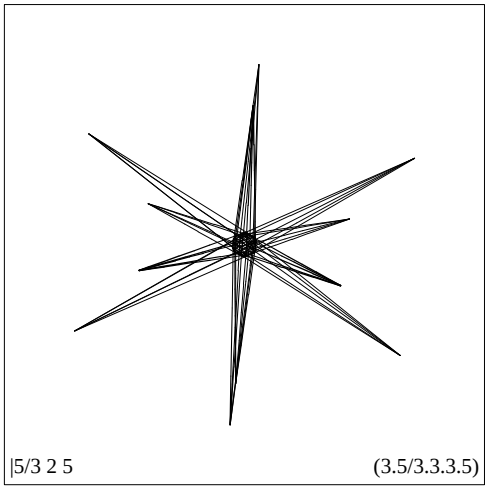

Fig. 65*

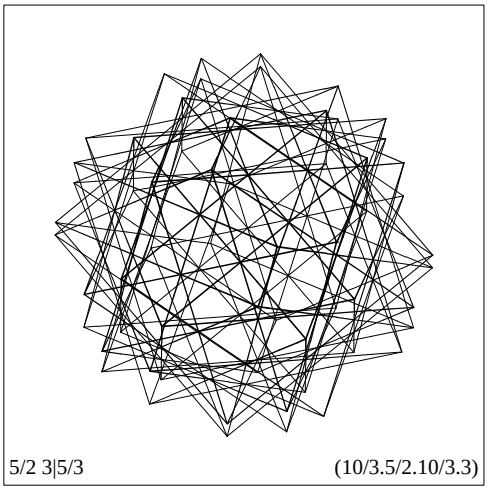

Fig. 66

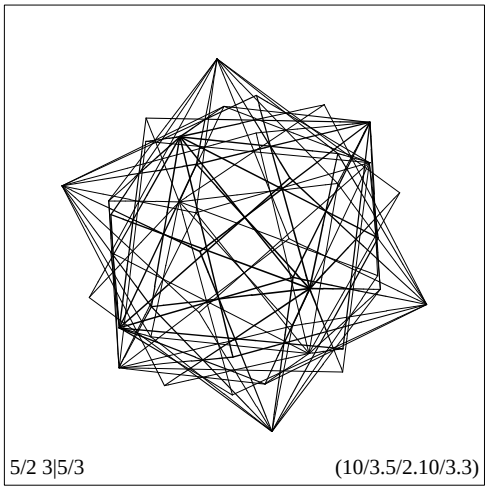

Fig. 66*

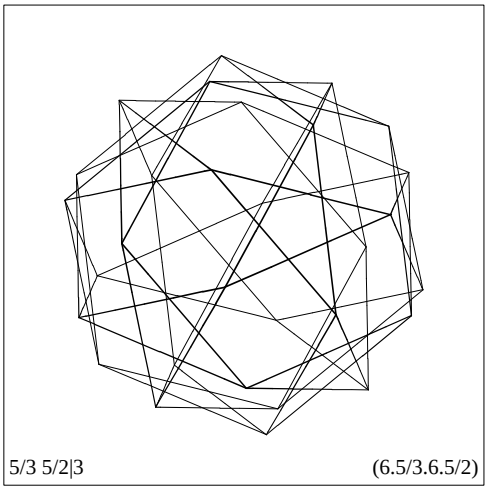

Fig. 67

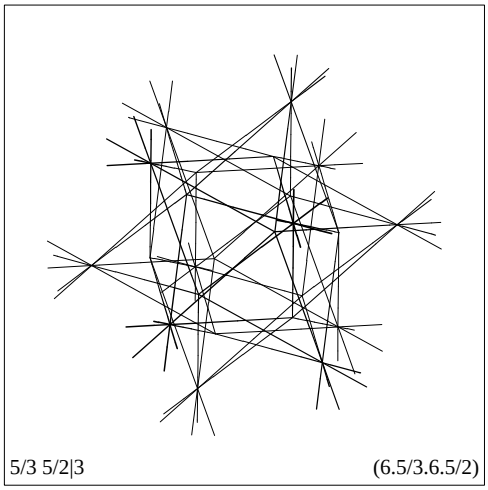

Fig. 67*

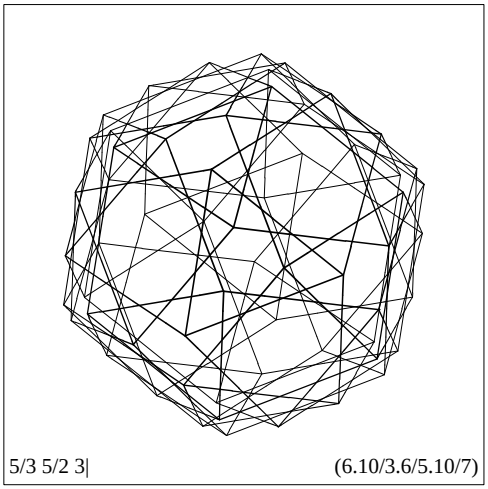

Fig. 68

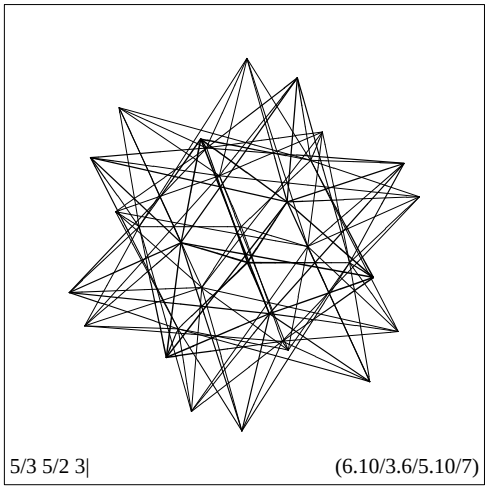

Fig. 68*

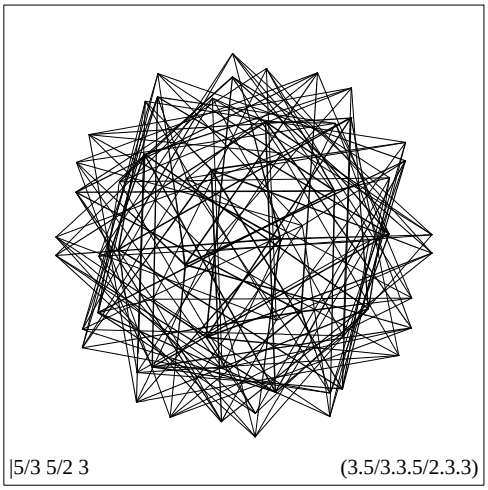

Fig. 69

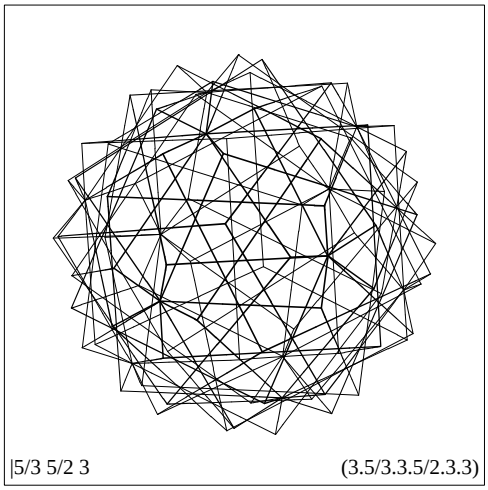

Fig. 69*

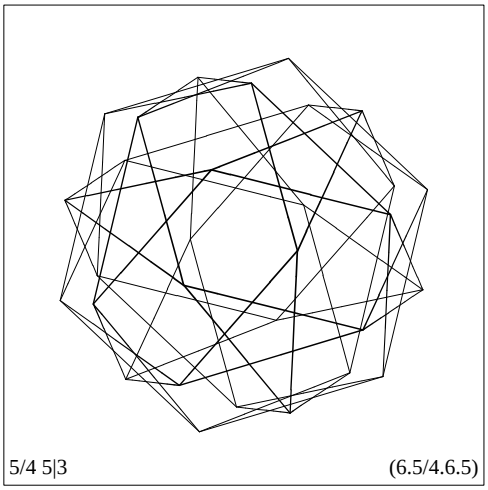

Fig. 70

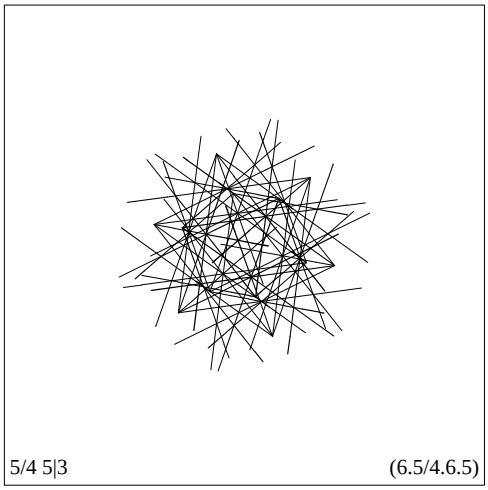

Fig. 70*

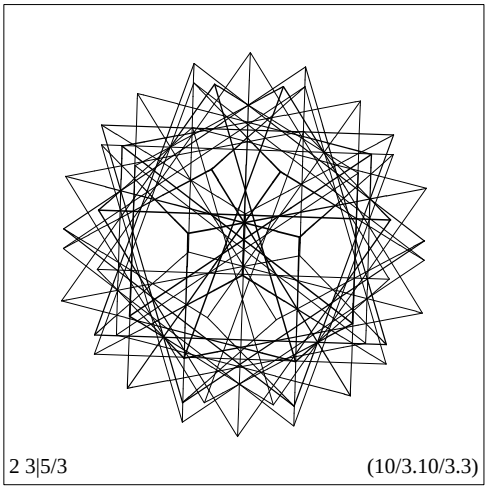

Fig. 71

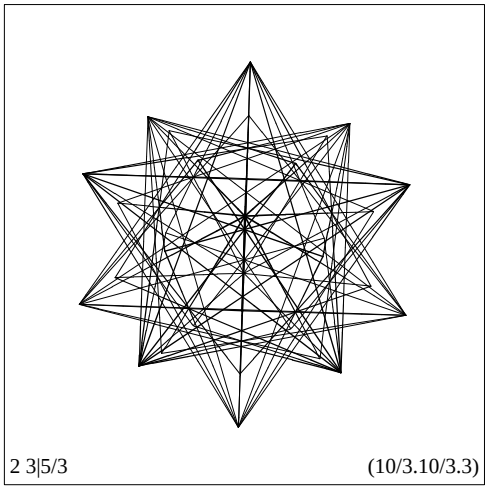

Fig. 71*

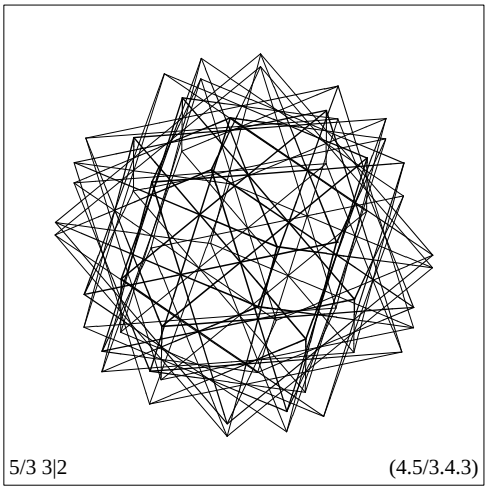

Fig. 72

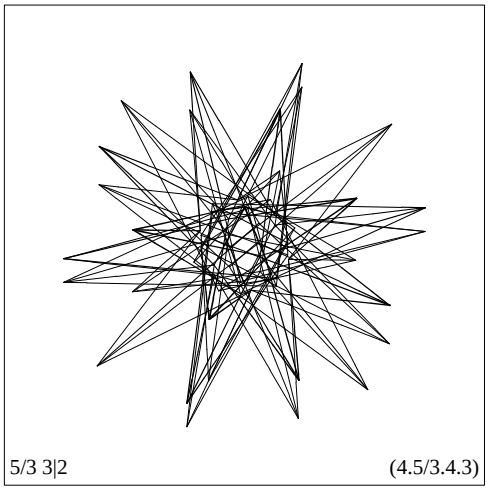

Fig. 72*

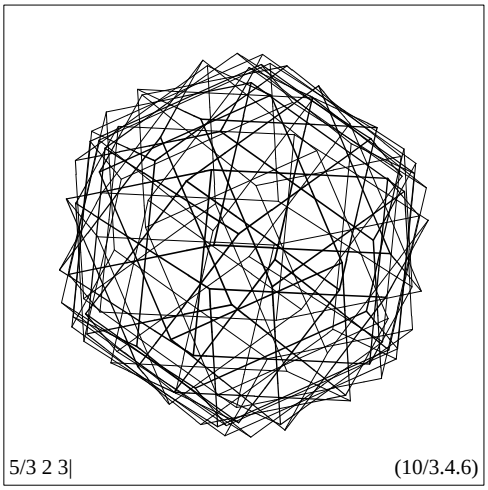

Fig. 73

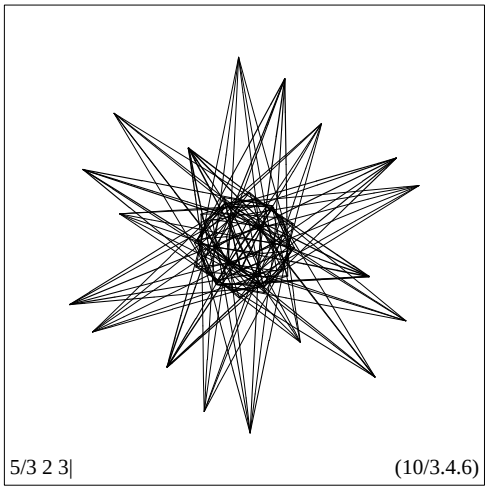

Fig. 73*

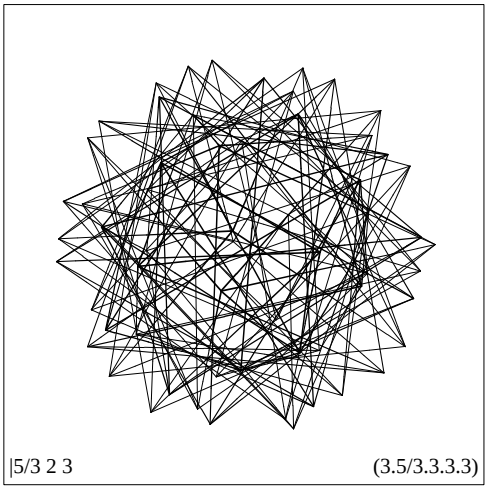

Fig. 74

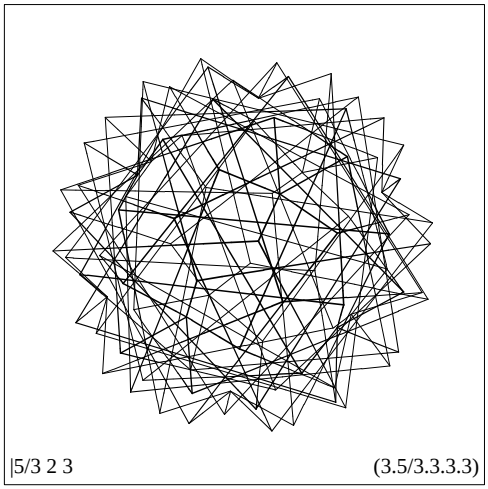

Fig. 74*

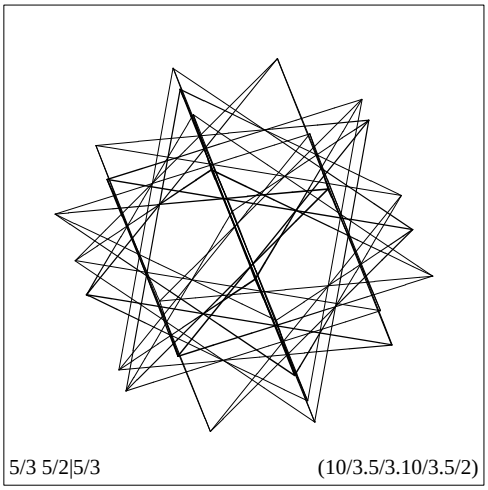

Fig. 75

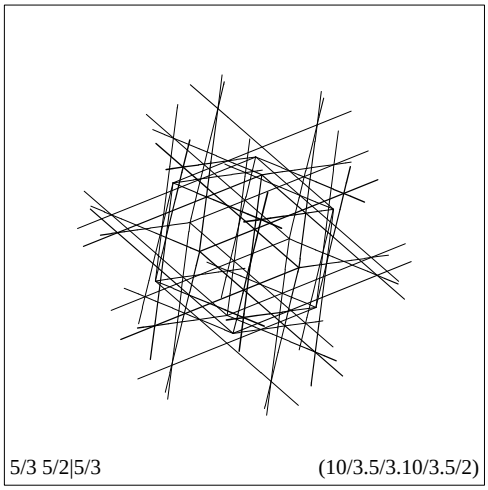

Fig. 75*

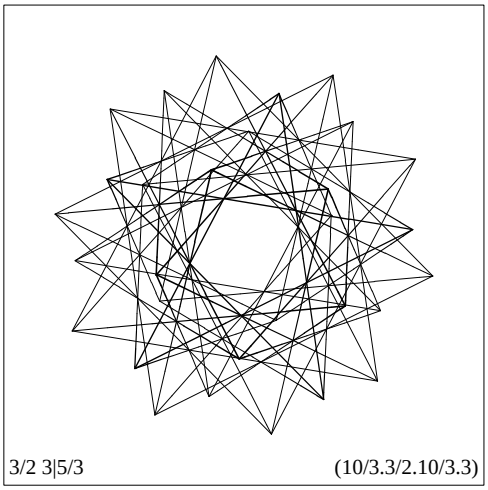

Fig. 76

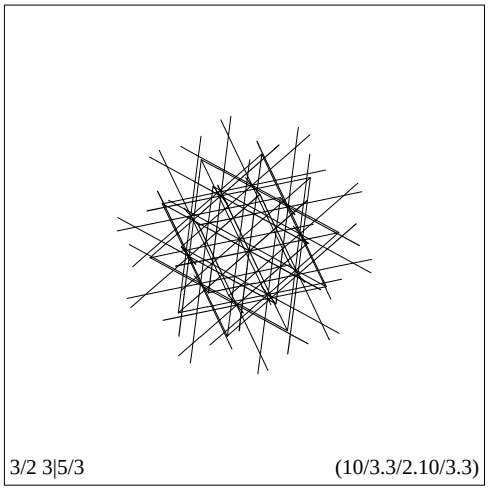

Fig. 76*

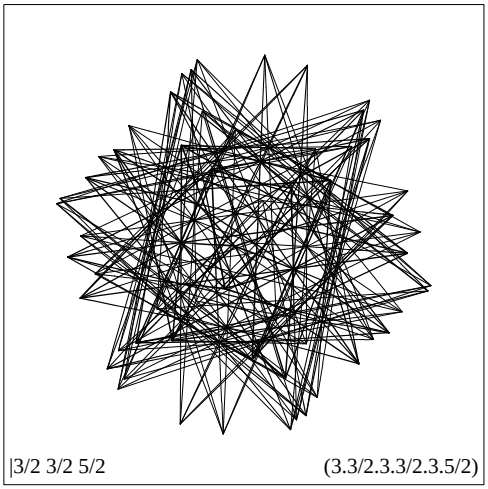

Fig. 77

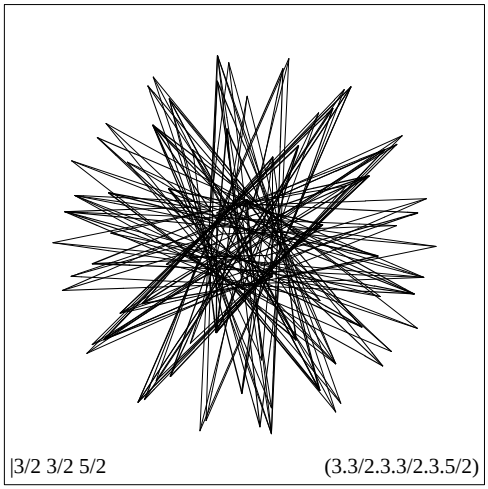

Fig. 77*

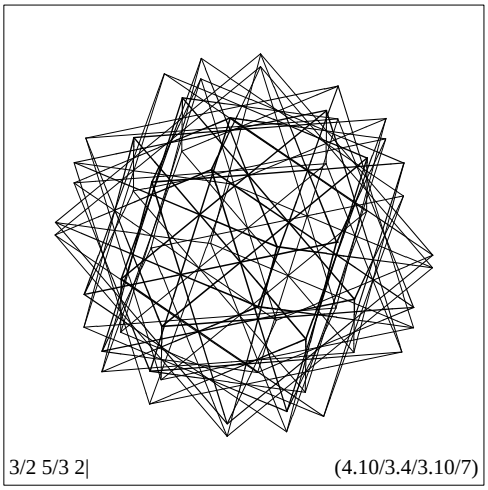

Fig. 78

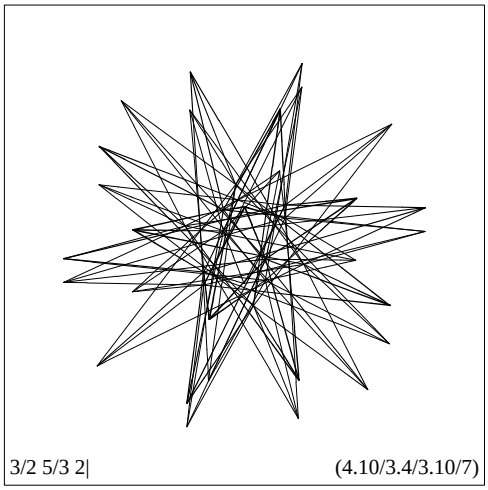

Fig. 78*

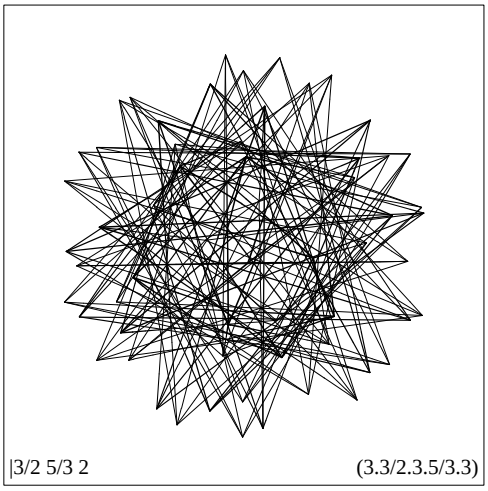

Fig. 79

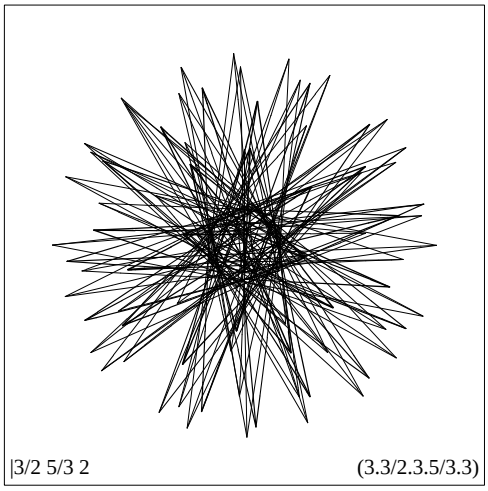

Fig. 79*

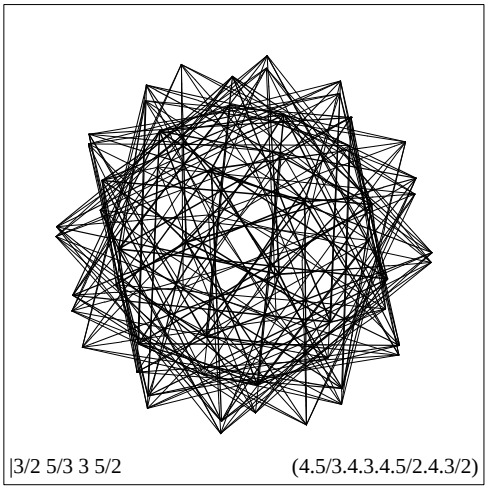

Fig. 80

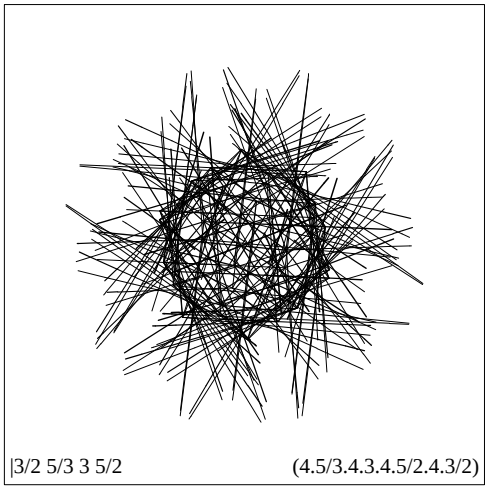

Fig. 80*